

# A direct transition between a Neel ordered Mott insulator and a $d_{x^2-y^2}$ superconductor on the square lattice

Ying Ran,<sup>1,2</sup> Ashvin Vishwanath,<sup>1,2</sup> and Dung-Hai Lee<sup>1,2</sup>

<sup>1</sup>*Department of Physics, University of California at Berkeley, Berkeley, CA 94720, USA*

<sup>2</sup>*Material Science Division, Lawrence Berkeley National Laboratory, Berkeley, CA 94720, USA*

(Dated: October 27, 2018)

In this paper we study a bandwidth-controlled direct, continuous, phase transition from a Mott insulator, with easy plane Neel order, to a fully gapped  $d_{x^2-y^2}$  superconductor with a doubled unit cell on the square lattice, a transition that is forbidden according to the Landau paradigm. This transition is made possible because the vortices of the antiferromagnet are charged and the vortices of the superconductor carry spins. These nontrivial vortex quantum numbers arise because the ordered phases are intimately related to a topological band insulator. We describe the lattice model as well as the effective field theory.

PACS numbers:

One of the central questions in the theory of the high  $T_c$  cuprates is how the antiferromagnetic (AF) insulator is converted into a d-wave superconductor (SC) upon doping. If a continuous transition between these, in some sense, diametrically opposite phases could be realized, it would be possible to construct an unified description of the SC and AF in terms of a single critical theory<sup>1</sup>.

An immediate indication that such a theory would be rather unconventional, is that it violates the ‘Landau’ rules which dictates that continuous phase transitions are only possible when the symmetry groups of the two phases have a subgroup relationship. It has been recently proposed that Landau forbidden transitions could in principle occur in quantum systems<sup>2</sup>, via ‘deconfined’ quantum critical points. In this area, early work on the AF to valence bond solid transition on the square lattice<sup>2,3</sup> has been generalized to a number of other transitions<sup>4,5,6,7</sup>. However, except an early numerical claim<sup>8</sup>, the physically most interesting case of a direct transition between an AF insulator and a SC has not been discussed before. Here, we provide a theory for such a transition.

The essential physics here is that vortices of the AF (in our case the easy-plane variety) are charged and the vortices of the SC carry spin. The condensation of either type of vortices drives the system between the two phases. The reason that the topological defects of these two rather conventional phases carry unconventional quantum numbers is because both phases are intricately related to a topological band insulator. The later is a special type of band insulator which can be differentiated from conventional ones by a topological quantum number.

The field theory that emerges at criticality is the easy plane version of the non-compact  $CP_1$  (NCCP<sub>1</sub>) model<sup>2,9</sup>. An important theoretical feature is that in contrast to most earlier theories<sup>4,5</sup> there is no emergent  $U(1)$  symmetry at criticality. An interesting critical point between an magnetic insulator and a d-wave SC with nodal quasiparticles was proposed in Ref.<sup>1</sup>. However, in contrast to the present theory, it is hard to establish that

the insulating state is truly an antiferromagnet.

In contrast to the cuprates, where the transition is triggered by doping, here we consider a bandwidth controlled Mott transition, where the system remains at half filling throughout. Moreover, in addition to the usual d-wave symmetry, our SC breaks lattice translation and time reversal symmetry due to a staggered spin dependent hopping term. This leads to a gap appearing at the nodes. Doping triggers a gap closing transition and gap nodes are restored at sufficiently high doping. Finally, our AF phase has a spin anisotropy favoring easy plane magnetic order. Topological defects with nontrivial quantum numbers were also discussed in Ref.<sup>10,11,12</sup>, in the context of cuprate superconductors.

While in mean-field theory the easy-plane NCCP<sub>1</sub> model clearly predicts a continuous transition, the effect of fluctuations has been actively debated<sup>9,13,14,15,16,17</sup>. If we consider the general family NCCP<sub>n</sub> models, these are known to have continuous transitions for  $n = 0$  and  $n \rightarrow \infty$ . For the case of  $n = 1$ , with full  $SU(2)$  symmetry, the case for a continuous transition has been made in some microscopic realizations<sup>14,15,16</sup>, although other authors have concluded that weak first order transitions are present in the entire parameter range<sup>17</sup>. Since the nature of the transition depends on the microscopic realization, it is clear that more numerical studies on a variety of models, including those with easy plane symmetry, are required to settle this question conclusively. In this paper, we do not further address this issue, rather we aim at establishing whether a continuous phase transition between the d-wave SC and AF insulator that is possible even in principle.

The plan of the paper is as follows. We start with the Bogoliubov-de Gennes description of a  $d_{x^2-y^2}$  superconductor with a particular unit cell doubling shown in Fig. 1 (see later) which leads to gapped nodes. It turns out that this is a topological superconductor, which in the presence of particle-hole symmetry, has stable edge modes. We show that vortices of this superconductor carry spin and are bosons. We ask what happens if these vortices condense. This is answered by studying the field

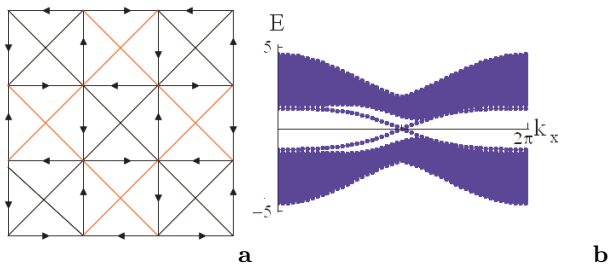


FIG. 1: (a) The arrows indicate the direction in which the nearest neighbor hopping amplitude is  $e^{i\phi}$  (hopping in the reverse direction has amplitude  $e^{-i\phi}$ ). The color indicates the sign of the next nearest neighbor hopping, Red means negative. (b) Bulk and edge spectra of Eq. (1) and Eq. (2). We used parameters  $\phi = \pi/5$  and  $t = 0.2$  (see the discussions below Eq. (1)).

theory of the vortex excitations, which predicts that the vortex condensed phase is an easy-plane antiferromagnet and the critical theory is an easy plane NCCP<sub>1</sub> model. A duality transformation allows us to study the transition in reverse, where condensation of charged vortices of the AF order leads to superconductivity. The self-duality of the NCCP<sub>1</sub> model<sup>9</sup> leads to an interesting spin-charge duality, whose consequences are described in Section IV A. As a consistency check, we study the same problem from the insulating side. Quite interestingly the most natural slave boson formulation leads to the same phase diagram and critical theory. This alternative approach also clarifies the role of symmetries required to realize this transition, and allows us to generalize this to other lattices. In the conclusion we discuss the similarity of the phenomenon described in this work and that of the cuprate superconductors. Eight appendices contain the important technical details of various parts of the paper, including Appendix F where the nature of the magnetic order are studied in details and Appendix H describes an equivalent theory on the honeycomb lattice, where a transition between an easy plane AF and a *triplet* superconductor occurs.

## I. THE TOPOLOGICAL D-WAVE SUPERCONDUCTOR

Let us begin with a mean-field description of one side of the phase transition: the d-wave superconductor. The usual d-wave superconductor has gapless nodal quasiparticles; here we introduce a modification which leads to a unit cell doubling, and a full gap around the Fermi surface. The mean-field Hamiltonian describing this superconductor is given by

$$\begin{aligned}
 H^{SC} &= \sum_{\langle ij \rangle \sigma} \text{Re}(\chi_{ij}) c_{i\sigma}^\dagger c_{j\sigma} - \sum_{\langle\langle ij \rangle\rangle \sigma \sigma'} \eta_i \text{Im}(\chi_{ij}) \epsilon_{\sigma\sigma'} c_{i\sigma} c_{j\sigma'} \\
 &+ \sum_{\langle\langle ij \rangle\rangle \sigma} \sigma t_{ij} c_{i\sigma}^\dagger c_{j\sigma} + h.c. \quad (1)
 \end{aligned}$$

Here  $i, j$  run through the sites of a square lattice,  $\eta_i$  is the AF staggered sign, and  $\langle ij \rangle, \langle\langle ij \rangle\rangle$  denote the nearest and second neighbors, respectively;  $\chi_{ij} = e^{\pm i\phi}$  and  $t_{ij} = \pm t$  ( $t = \text{real}$ ). We note, the nearest neighbor hopping,  $\text{Re}(\chi_{ij})$ , is the same as the hopping parameter associated with the “staggered flux phase” of the Heisenberg antiferromagnet<sup>18</sup> (for a review, see Ref.<sup>19</sup>). We illustrate the  $\chi_{ij}$  and  $t_{ij}$  patterns in Fig(1(a)). It is important to note that the pairing term has  $d_{x^2-y^2}$  symmetry; due to the presence of  $\eta_i$  in the second term of Eq. (1), the pairing is translation-invariant.

However, because of the spin-dependent second neighbor hopping, both lattice translation  $T$  and time reversal  $\mathcal{TR}$  are broken. However,  $T \circ \mathcal{TR}$  and reflection along the vertical (horizontal) line passing the center of each plaquette ( $\mathcal{P}$ ) are symmetries of the Hamiltonian. ((By looking at Fig(1(a)) one might think that reflection is not a symmetry. However this figure merely illustrates the pattern of  $\chi_{ij}$  and  $t_{ij}$  not the symmetry of the Hamiltonian.) In addition, Eq. (1) has spin  $S_z$  rotation symmetry, and the charge  $U(1)$  symmetry is, of course, spontaneously broken.

We will see in later discussions that  $T \circ \mathcal{TR}$  and  $\mathcal{P}$  together with the  $U(1) - S_z$  conservation and the  $U(1)$ -charge conservation (which is spontaneously broken in the current superconductor phase), ensures that the direct SC $\leftrightarrow$ AF transition can be continuous at half-filling. There are two more symmetries of the Hamiltonian Eq. (1) which simplify our analysis but are not necessary for the direct transition to occur: the particle hole conjugation  $PH$  ( $c_{i\uparrow} \rightarrow \eta_i c_{i\downarrow}^\dagger, c_{i\downarrow} \rightarrow -\eta_i c_{i\uparrow}^\dagger$ ) and translation together with  $c_{i\sigma} \leftrightarrow c_{i-\sigma}$  ( $T \circ \uparrow \leftrightarrow \downarrow$ ).

Eq. (1) is closely related to a special type of topological insulator (TBI) Hamiltonian

$$H^{TBI} = \sum_{\langle ij \rangle, \sigma} \chi_{ij} f_{i\sigma}^\dagger f_{j\sigma} + \sum_{\langle\langle ij \rangle\rangle, \sigma} \sigma t_{ij} f_{i\sigma}^\dagger f_{j\sigma} + h.c.. \quad (2)$$

Indeed, one can transform Eq. (1) into Eq. (2) by making the following transformation

$$c_{i\uparrow} = e^{i\frac{\pi}{4}} \left( \frac{f_{i\uparrow} - \eta_i f_{i\downarrow}^\dagger}{\sqrt{2}} \right), \quad c_{i\downarrow} = e^{i\frac{\pi}{4}} \left( \frac{f_{i\downarrow} + \eta_i f_{i\uparrow}^\dagger}{\sqrt{2}} \right). \quad (3)$$

If we drop the  $\sigma$  in front of the  $t_{ij}$ , Eq. (2) turns into the Hamiltonian for the “chiral spin liquid”<sup>20</sup>. With the  $\sigma$ , the chirality of the spin up and spin down fermions are opposite. In that case Eq. (2) describes a band insulator with opposite “TKNN index”<sup>21</sup> ( $\pm 1$ ) for the spin up/down fermions. Hence this type of topological insulator will exhibit the spin hall effect. However, unlike the spin hall insulator introduced in Ref.<sup>22</sup>, our spin hall insulator breaks time reversal symmetry. (To appreciate the full relationship between Eq. (1) and Eq. (2), see Sec. V)

Since Eq. (3) is a unitary transformation the excitation spectra of Eq. (2) and Eq. (1) are the same. One only needs to reinterpret the electron/hole excitations in

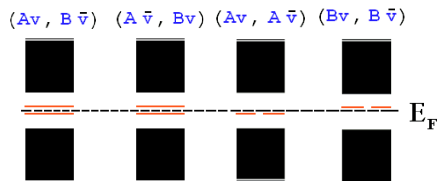


FIG. 2: The Bogoliubov quasiparticle (q.p.) spectra of a pair vortex and anti vortex; The red lines mark the core states, and the black solid line represents the Fermi energy. In the limit of infinite vortex-antivortex separation each core level is doubly degenerate. We used parameters  $\phi = \pi/5$  and  $t = 0.2$  (see the discussions below Eq. (1)).

the TBI as the Bogoliubov quasiparticle excitations in the superconductor. Interestingly, the conserved  $S_z$  of Eq. (2) translates into conserved  $S_z$  of Eq. (1) as well. Among other things the above correspondence implies that the superconductor described by Eq. (1) has gapless edge excitations (Fig.1(b)). Thus it is justified to regard this type of superconductor as “topological”. In Appendix G 2 and near the end of Sec.V B we show that the edge modes requires the  $PH$  symmetry which is difficult to realize in a material. Therefore in general there is no gapless edge modes and the SC phase is not topological. On the other hand the physics of the direct  $SC \leftrightarrow AF$  transition, which is the main result of the current paper, does not require the existence of gapless edge modes.

Now let us study the vortices of the superconductor. Direct numerical calculations for a vortex and antivortex pair gives the spectra illustrated in Fig.(2), where each core level is doubly degenerate (in the limit of infinite separation between the vortices)/ There AV and  $B\bar{V}$  stand for a vortex located on A dual sublattice and an antivortex on B dual sublattice, and etc. Here A/B dual sublattice locate at the center of plaquette in Fig.(1(a)) marked by red/black cross lines. The core levels of these two types of vortices lie on opposite side of zero. In the ground state all levels below/above zero are filled/empty. For each vortex/antivortex, there are three low lying excited states arise from different way of occupying the two core levels associated with it. Explicit calculation of the ground state value of  $S_z$  associated with the four panels of Fig.(2) gives

$$S_{AV}^z = S_{A\bar{V}}^z = 1/2, \text{ and } S_{B\bar{V}}^z = S_{BV}^z = -1/2. \quad (4)$$

The spin distribution associated with  $(AV, A\bar{V})$  and  $(AV, B\bar{V})$  is shown in Fig.(3).

The fact that vortices carry spins is the most interesting aspect of the superconductor under consideration.

In the above numerical study, the size of the vortex core (the region in which the pairing amplitude is suppressed to zero) is one lattice constant. As the core size of the

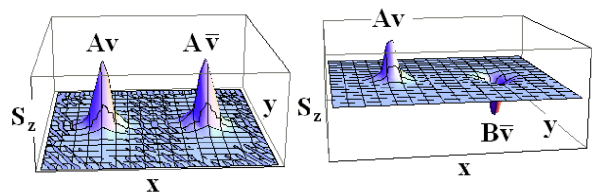


FIG. 3: The  $S_z$  distribution of an  $(AV, A\bar{V})$  and  $(AV, B\bar{V})$  pair. The total integrated values of  $S_z$  around each vortex is  $S_z = \pm 1/2$ .

vortices increase, their core levels move toward zero. As the core size diverge, a continuum BdG equation applies. In that limit all core levels are situated at zero energy (Appendix B) and the previous three (low lying) excited states become degenerate with the ground state. When that happen it is no longer possible to differentiate the spectrum of A and B dual sublattice vortices. In this limit each vortex/antivortex has four degenerate states: two with  $S_z = \pm 1/2$  and the other two with spin zero.

Next we determine the statistics of the vortices. For this purpose it is important to note that under

$$\begin{aligned} PH: AV_\uparrow &\leftrightarrow A\bar{V}_\uparrow, BV_\downarrow \leftrightarrow B\bar{V}_\downarrow \\ T \circ \mathcal{TR}: AV_\uparrow &\leftrightarrow B\bar{V}_\downarrow, BV_\downarrow \leftrightarrow A\bar{V}_\uparrow \end{aligned} \quad (5)$$

Now let  $\phi_{BV_\downarrow, BV_\downarrow}$ , and etc., be the phase factor due to the (counterclockwise) exchange of two  $BV_\downarrow$  vortices.  $T \circ \mathcal{TR}$  plus PH imply  $\phi_{BV_\downarrow, BV_\downarrow} = \phi_{AV_\uparrow, AV_\uparrow}^*$ . On the other hand,  $T \circ \uparrow \leftrightarrow \downarrow$  requires  $\phi_{BV_\downarrow, BV_\downarrow} = \phi_{AV_\uparrow, AV_\uparrow}$ . Put together the above implies  $\phi_{AV_\uparrow, AV_\uparrow}^* = \phi_{AV_\uparrow, AV_\uparrow}$ . Consequently

$$\phi_{AV_\uparrow, AV_\uparrow} = \pm 1, \quad (6)$$

i.e.,  $AV_\uparrow$  is either boson or fermion (the same for  $BV_\downarrow$ ). Although we used the symmetry  $T \circ \uparrow \leftrightarrow \downarrow$  to derive this result, the result Eq.(6) does not depend on that symmetry because statistics cannot change so long as the core levels do not merge into the continuum.

To further distinguish the two we consider the following gauge transformation  $c_{i\sigma} \rightarrow e^{i\theta_i/2} c_{i\sigma}$ . This transformation remove the vorticity in the pairing order parameter up to a  $\pi$  cut. The hopping parameters acquires a  $\pi$  cut as well as a smooth hopping phase  $e^{i\alpha_{ij}}$  where  $\alpha_{ij} = \text{Mod}(\frac{\theta_i - \theta_j}{2}, \pi)$ . This hopping phase is often referred to as the “Doppler shift term” in the theory of superconductivity. If one gets rid of the hopping phase, and leaves the  $\pi$  cut in both the pairing and hopping parameters, both core levels of a given vortex/antivortex move to zero energy and there are four degenerate vortex states, like the case of the diverging core size discussed earlier. In Fig.(4) we illustrate the evolution of the spectra for a  $AV_\uparrow$  and a  $B\bar{V}_\downarrow$  vortex after the following modification of the hopping phase:

$$e^{i\alpha_{ij}} \rightarrow e^{i\lambda\alpha_{ij}} \quad 0 \leq \lambda \leq 1. \quad (7)$$

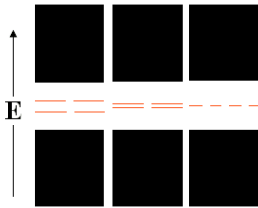


FIG. 4: The spectra of a  $AV_{\uparrow}$  and a  $B\bar{V}_{\downarrow}$  vortex as a function of  $\lambda$ . From left to right  $\lambda = 1, \frac{1}{2}$  and 0.

In the  $\lambda = 0$  limit Eq. (3) transforms Eq. (1) to a spin-Hall insulator with  $Z_2$  flux in the plaquette previously occupied by the vortices. This is a problem we have previously solved and the  $S_z = \pm 1/2$  vortices (which are referred to as spin fluxons in Ref.<sup>23</sup>) are bosons<sup>23</sup>. It is simple to show that Eq. (5) holds true for all  $\lambda$  hence Eq. (6) remains valid. This, plus the fact that the spin fluxons adiabatically evolve into the spin-carrying vortices, implies

$$\phi_{AV_{\uparrow}, AV_{\uparrow}} \Big|_{\lambda=1} = 1, \quad (8)$$

, i.e., the  $AV_{\uparrow}$  vortices are bosons (same argument applies to  $BV_{\downarrow}$ ,  $A\bar{V}_{\uparrow}$  and  $B\bar{V}_{\downarrow}$ .)

---


$$\mathcal{L} = \sum_{\sigma} \left\{ \sum_{\mu} |(\partial_{\mu} + i\alpha_{\mu} - i\frac{\hbar}{2} A_{\mu}^S \sigma^3) \Psi_{\sigma}|^2 + m^2 |\Psi_{\sigma}|^2 \right\} + v(\sum_{\sigma} |\Psi_{\sigma}|^2)^2 + u|\Psi_{\uparrow}|^2 |\Psi_{\downarrow}|^2 + \frac{\kappa}{2} (\nabla \times \alpha)^2 + \frac{ie}{\pi} A \cdot (\nabla \times \alpha) \quad (9)$$


---

Where  $\Psi_{\uparrow}, \Psi_{\downarrow}$  are relativistic vortex fields, and for brevity, we have omitted the space-time dependence of all fields. In addition, we have used a three vector notation  $\nabla = (\partial_0, \Delta_x, \Delta_y)$  to denote space time derivatives. The connection between these relativistic fields and the microscopic vortex fields is discussed in Appendix A. As usual, a gauge field  $\alpha$  is introduced such that  $\frac{2e}{2\pi} \nabla \times \alpha =$  is the Cooper pair 3-current caused by the gaussian fluctuations of the pair-condensate phase. Hence, it is coupled to the external electromagnetic field  $A$ , contained in the last term of Eq. (9). The minimum coupling  $\sum_{\mu} |(\partial_{\mu} + i\alpha_{\mu} - i\frac{\hbar}{2} A_{\mu}^S \sigma^3) \Psi_{\sigma}|^2$  between  $\Psi_{\sigma}$  and  $\alpha_{\mu}$  reflects the fact that vortices see the 3-current of the condensate as electric and magnetic fields. To probe the spin response we have we coupled a “spin gauge field”  $A_{\mu}^S$  to the conserved  $S_z$  current. Note that both  $A_{\mu}$  and  $A_{\mu}^S$  are non-dynamical. The fact that the vortices minimally couple to the spin gauge field reflects the fact that they carry spin. The  $\frac{\hbar}{2} \sigma^3$  in the coupling between  $\Psi_{\sigma}$  and  $A_{\mu}^S$  reflects the fact that the  $\Psi_{\uparrow, \downarrow}$  boson carries  $S_z = \pm 1/2$ . Finally, we have included standard Ginzburg-Landau type quartic  $\Psi_{\sigma}$  terms. They describe the interaction between

## II. THE SUPERCONDUCTOR-VORTEX FIELD THEORY

Since the vortices are bosons, they can condense. The condensation will trigger the destruction of superconductivity and lead to an insulator. However, since the vortices carry spin, we expect the resulting insulator to have magnetic signature. To understand what happens after vortices have condensed, we examine the effective field theory describing the phase fluctuations of the superconductor. Phase fluctuations appears in two different types: gaussian (spin wave ) type and vortex-antivortex fluctuations. The latter is responsible for destroying the superconducting state when it is strong. For example, it is the vortex condensation that triggers the ordinary superconductor to insulator transition. A convenient way of describing the vortex physics is to use the dual form of the phase fluctuation theory<sup>24,25</sup>. In this form, the vortices are particles and the original boson density and current become magnetic and electric fields respectively. Since this dual form is widely used in literature, we will refer the readers to references<sup>24,25</sup> for details. The relevant field theory for the superconducting vortices in three dimensional Euclidean space takes the form:

---

the order parameters of the two type of vortices.

To ensure the correctness of the low energy effective theory Eq.(9), the following conditions must be met: (1)  $\Psi_{\uparrow} \rightarrow \Psi_{\downarrow}$  symmetry (the two boson fields are interchangeable), (2)  $\Psi \rightarrow \Psi^{\dagger}$  symmetry (particle and anti-particle are on the same footing which requires the effective theory to be relativistic), (3)  $\Psi$  particles do not experience a background magnetic field; i.e. there is no linear term  $\hbar(\partial_x \alpha_y - \partial_y \alpha_x)$  in the action above. We show in the following that the three requirements are ensured by the symmetry operations  $PH$ ,  $\mathcal{P}$  and  $T \circ \mathcal{TR}$ . (Eventually, in Sec.VII, we will show that even  $PH$  is not required: as long as the density is fixed at half-filling, the low energy effective theory Eq.(9) is correct.)

Note that according to Eq.(5) both  $PH$  and  $\mathcal{P}$  transforms a vortex into an anti-vortex, while preserving spin while  $T \circ \mathcal{TR}$  transforms a vortex into an anti-vortex and

flips spin. Therefore,

$$PH: \Rightarrow \Psi_{\uparrow} \rightarrow \Psi_{\downarrow}^{\dagger}, \Psi_{\downarrow} \rightarrow \Psi_{\uparrow}^{\dagger} \quad (10)$$

$$\mathcal{P}: \Rightarrow \Psi_{i\uparrow} \rightarrow \Psi_{\mathcal{P}(i)\downarrow}^{\dagger}, \Psi_{\downarrow} \rightarrow \Psi_{\mathcal{P}(i)\uparrow}^{\dagger} \quad (11)$$

$$T \circ \mathcal{TR}: \Rightarrow \Psi_{\uparrow} \rightarrow \Psi_{\uparrow}^{\dagger}, \Psi_{\downarrow} \rightarrow \Psi_{\downarrow}^{\dagger} \text{ (anti-unitary)} \quad (12)$$

Although  $\mathcal{P}$  and  $PH$  perform similar transformations on the vortex field, they act very differently on the background flux ( $\partial_x \alpha_y - \partial_y \alpha_x$ ).  $\mathcal{P}$  changes the sign of this term while  $PH$  leaves it invariant. Therefore the combination of  $\mathcal{P}$  and  $PH$  ensures condition (3). Similarly, Eq. (10) and Eq. (12) validate the conditions (1) and (2). Therefore in the presence of  $PH$ ,  $\mathcal{P}$  and  $T \circ \mathcal{TR}$  conditions (1),(2) and (3) are satisfied. This dictates the effective field theory above. In later discussions we will derive the same theory from a completely different approach Eq.(39). This will clarify the role of particle hole symmetry, which will not be necessary as a microscopic symmetry to achieve this transition. Note, in the absence of the external fields  $A$ ,  $A^S$  and in the presence of easy plane anisotropy ( $u < 0$ ), the above theory is identical to the easy plane NCCP<sub>1</sub> of Ref.<sup>9</sup>.

### III. THE AF ORDER IN THE VORTEX CONDENSED PHASE

Let us now focus on Eq. (9); for  $m^2$  large and positive, the  $\Psi_{\sigma}$  vortices are absent at long wavelength/time. In that limit Eq. (9) becomes a gaussian theory in  $\alpha_{\mu}$ . Integrating out  $\alpha_{\mu}$  generates a Higgs effective action for  $A_{\mu}$ , in other words, the system is a superconductor. When  $m^2$  changes sign the spin-carrying vortices will condense. If  $u > 0$  the  $\Psi_{\uparrow}$  and  $\Psi_{\downarrow}$  vortices suppress each other, hence energetically it is favorable for  $\langle \Psi_{\uparrow} \rangle \neq 0, \langle \Psi_{\downarrow} \rangle = 0$  or  $\langle \Psi_{\uparrow} \rangle = 0, \langle \Psi_{\downarrow} \rangle \neq 0$  in the condensed phase. When  $-4v < u < 0$  it is favorable for (1)  $\langle \Psi_{\uparrow} \rangle = \langle \Psi_{\downarrow} \rangle \neq 0$  or (2)  $\langle \Psi_{\uparrow}^{\dagger} \Psi_{\downarrow} \rangle \neq 0$  while  $\langle \Psi_{\uparrow} \rangle = \langle \Psi_{\downarrow} \rangle = 0$ . In case (2) the order parameter has no vorticity (hence is a local operator) while flips the spin. When it develops expectation value, superconductivity needs not be destroyed. Since  $\langle \Psi_{\uparrow}^{\dagger} \Psi_{\downarrow} \rangle \sim \langle S^+ \rangle \neq 0$ , the system exhibits SC and magnetic order simultaneously. While this scenario can certainly be realized in certain parameter regime, in the rest of the paper we focus on the more interesting case where the system goes from  $\langle \Psi_{\uparrow} \rangle = \langle \Psi_{\downarrow} \rangle = 0$  to  $\langle \Psi_{\uparrow} \rangle = \langle \Psi_{\downarrow} \rangle \neq 0$  in a single transition.

When single vortices condense, a SC turns into an insulator. When both  $\langle \Psi_{\uparrow} \rangle$  and  $\langle \Psi_{\downarrow} \rangle$  are non zero,  $\langle \Psi_{\uparrow}^{\dagger} \Psi_{\downarrow} \rangle$  hence  $\langle S^+ \rangle$  are also non vanishing. As a result, the insulating phase has easy plane magnetic order. However, what is the order pattern? Is it AF or ferromagnetic?

To minimize technical complexity, here we present a simple, but less rigorous, way to clarify the nature of the magnetic order. We put the more rigorous calculation,

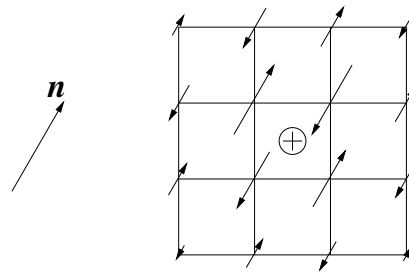


FIG. 5: For  $\text{Re}(\chi) = 1$ ,  $t = 0.8$ , and  $\text{Im}(\chi) = 0.3$  (see Eq.(1)) and a vortex located in the plaquette labeled by  $\oplus$ , we plot the magnetization  $\langle S_i^n \rangle$  on site  $i$  in a small in-plane field  $\vec{B} = 0.1\hat{n}$ . The sign of the magnetization is labeled by the arrows, and the length of the arrows is proportional to  $|\langle S_i^n \rangle|$ . The calculation is performed on a 1152-site system with one vortex and one anti-vortex separated by half system size.

based on computing vortex tunneling amplitude, in Appendix E. To mimic the coherent tunneling ( $\langle \Psi_{\uparrow}^{\dagger} \Psi_{\downarrow} \rangle \neq 0$ ) between the spin up and spin down vortex states in the magnetic phase, we turn on a small in plane magnetic field (the field strength needs to be larger than the spacing between the core levels in the first panel of Fig.2) to mix the spin-up and spin-down vortex states in a single static vortex. In Fig.5 we show the expectation value of the in-plane spin component in the vicinity of the vortex core when there is an in plane magnetic field in  $\hat{n}$  direction. The AF order is clearly seen.

### IV. TRANSITION FROM THE AF SIDE

In the previous section we have analyzed the SC  $\leftrightarrow$  AF transition from SC side using the effective action given in Eq.(9). In this section we approach the transition from the AF side, where the AF order is destroyed by the condensation of AF vortices. Since superconductivity emerges after this condensation, it suggests that the AF vortices carry electric charge. In the following we show that this is indeed the case.

Let us assume in vortex condensed phase the U(1) order parameter  $\langle \Psi_{\uparrow} \rangle$  and  $\langle \Psi_{\downarrow} \rangle$  have equal magnitude. In the following we derive an effective theory describing the vortices of these order parameter fields. The AF $\rightarrow$ SC transition is then triggered by the condensation of these new vortices. The derivation is accomplished by the performing duality transformation<sup>24,25</sup> on Eq.(9) (for details see appendix A). In fact, in the absence of the external gauge potentials  $A$ ,  $A^S$ , this has been carried out in Ref.<sup>9</sup> where it was discovered that the theory at criticality is self-dual. In appendix A we extend it to the case with these potentials present. The end result is the effective theory given in Eq. (13). Essentially in the AF phase described by  $\langle \Psi_{\uparrow} \rangle = \sqrt{\rho}e^{i\phi_{\uparrow}}$ ,  $\Psi_{\downarrow} = \sqrt{\rho}e^{i\phi_{\downarrow}}$ , there are two types of vortices. One causes the winding of  $\phi_{\uparrow}$  by  $2\pi$  and the other the winding of  $\phi_{\downarrow}$  by  $-2\pi$  (here the minus sign is chosen for convenience). In the presence of

such vortices,  $\alpha$  nucleates  $\pm\pi$  fluxes to screen the vorticity (so that the kinetic energy is minimized). From the term  $i\frac{e}{\pi}A \cdot \nabla \times \alpha$  in Eq. (9) we find that these two types of screened vortices carry charge  $\pm e$ . We label these vortices by  $z_1$  and  $z_2$  respectively. This explains the opposite sign in the minimal coupling to  $\mathbf{A}$  in the first term of Eq. (13). The curl of the  $a_\mu$ , namely  $\nabla \times \mathbf{a}$ , describes the spin 3-current caused by the gaussian fluctuation in

---


$$\mathcal{L}_{\text{dual}} = \sum_{\alpha=1}^2 \left[ \sum_{\mu} |(\partial_{\mu} + ia_{\mu} - ieA_{\mu}\sigma^3)z_{\alpha}|^2 + m^2|z_{\alpha}|^2 \right] + u|z_1|^2|z_2|^2 + v \left( \sum_{\alpha} |z_{\alpha}|^2 \right)^2 + \frac{\kappa}{2}(\nabla \times \mathbf{a})^2 + c_1(\nabla \times A)^2 - \frac{i\hbar}{2\pi}(\nabla \times \mathbf{a}) \cdot A^S \quad (13)$$

Note, the form of Eq. (13) is almost identical to Eq. (9) except for the exchange  $\Psi_{\sigma} \leftrightarrow z_{\alpha}$  and  $2eA \leftrightarrow \hbar A^S$ . Since Eq.(13) is the dual theory of Eq.(9), it must be consistent with microscopic symmetries of Eq.(9). In Appendix G 1 we further directly checked the consistency between microscopic symmetries and Eq.(13).

Next let us how to describe the magnetically ordered phase using Eq. (13). In the  $\langle \psi_{\sigma} \rangle \neq 0$  phase,  $m^2 > 0$  and the  $z_{\alpha}$  bosons are absent at long wavelength/time. In that limit we again have a gaussian theory

$$\mathcal{L}_{\text{gauge}} \rightarrow \frac{\kappa}{2}(\nabla \times \mathbf{a})^2 - \frac{i\hbar}{2\pi}A^S \cdot \nabla \times \mathbf{a}. \quad (14)$$

describing a ‘‘spin superfluid’’. The above action is dual to the following Goldstone action

$$\mathcal{L}_{\text{GS}} = \frac{1}{2\kappa} \sum_{\mu} (\partial_{\mu}\chi - \hbar A_{\mu}^S)^2. \quad (15)$$

Here the phase angle  $\chi$  transforms under a angle  $\beta$ - $S_z$  rotation as  $\chi \rightarrow \chi + \beta$ . It can also be shown that computing the spin-spin correlation function  $\langle e^{i\chi(\mathbf{x}_1,t)} e^{-i\chi(\mathbf{x}_2,t)} \rangle$  using action Eq. (15) is equivalent to computing the monopole-anti monopole correlation function using Eq. (14), i.e.,

$$\langle e^{i\chi(\mathbf{x}_1,t)} e^{-i\chi(\mathbf{x}_2,t)} \rangle_{\mathcal{L}_{\text{GS}}} = \langle V^+(\mathbf{x}_1,t) V^-(\mathbf{x}_2,t) \rangle_{\mathcal{L}_{\text{gauge}}} \quad (16)$$

Here  $V^+$  and  $V^-$  are the creation operators of the monopole and antimonopole in  $a$ -gauge field. Since a monopole (anti-monopole) is the event at which  $\frac{1}{2\pi}(\nabla \times \mathbf{a})_0 = S_z/\hbar$  changes by 1 ( $-1$ ), we conclude that

$$\langle V^+(\mathbf{x}_1,t) V^-(\mathbf{x}_2,t) \rangle \sim \langle S^+(\mathbf{x}_1,t) S^-(\mathbf{x}_2,t) \rangle. \quad (17)$$

Thus the  $S_z$  spin superfluid described by Eq. (14) and Eq. (15) is an XY ordered magnet (from the previous discussion we know this order is AF) and  $z_1^{\dagger}, z_2^{\dagger}$  create charged XY vortices (anti-vortices). Finally  $z_1^{\dagger} z_2$  inserts

the phase of  $\langle S^- \rangle \sim e^{i(\phi_{\uparrow} - \phi_{\downarrow})}$ . This is reflected in the last term of Eq. (13). Since both  $z_1$  and  $z_2$  creates  $2\pi$  winding in  $\phi_{\uparrow} - \phi_{\downarrow}$  it couples to  $a_{\mu}$  minimally as shown by the first term of Eq. (13). Finally  $z_1^{\dagger} z_2$  inserts charge  $2e$  while has no spin vorticity (hence is a local operator) is the Cooper pair operator.

---

charge  $2e$  hence creates a monopole in  $a$ -gauge field, and  $\Psi_{\uparrow}^{\dagger} \Psi_{\downarrow}$  raise  $S_z$  by 1 hence is a monopole operator  $V^{\dagger}$  in  $a$ -gauge field. (We will come back to this point later in the slave-rotor description Sec.V and Sec.F, where we explicitly compute the monopole quantum number for  $V^{\dagger}$  and find it is AF.)

Since  $z_1$  and  $z_2$  carry the vorticity of magnetic order parameter their condensation will destroy the AF order. However since  $z_1$  and  $z_2$  carry charge, the condensate is a superconductor. Now we have gone through a full circle. We start from the d-wave superconductor, the spin-carrying vortex condensation brings the system to a XY ordered antiferromagnet. In the reverse direction, start from the antiferromagnet, the condensation of the charge-carrying vortices brings the system back to the superconductor.

In Lapp.D,E we perform the parallel study of the AF vortex core states as what we did for SC vortex in Sec.I,II,III. We indeed find that there are two mid-gap levels in the AF vortex core. The filling/unfilling of these levels lead to charge- $\pm 1$  AF vortices, whose condensation triggers the SC order. Analogous to the discussion in section III we can determine the SC pairing symmetry by studying the tunneling property of the magnetic vortices.

## A. Spin-Charge Duality

As mentioned previously, the self duality of the easy plane NCCP<sub>1</sub> model at criticality, leads to spin-charge duality here. The effective theories near the transition point, Eq. (9) and Eq. (13), map onto one another with the substitution  $\Psi_{\sigma} \leftrightarrow z_{\alpha}$ ,  $2eA \leftrightarrow \hbar A^S$  which implies that the roles of spin and charge are identical at criticality. We point out some consequences of this duality in the following.

At criticality we expect both the electric and spin conductivity to be finite and nonzero. The self duality en-

sures the electric conductivity ( $\sigma_c$ ) and spin conductivity ( $\sigma_s$ ) to be related by  $\frac{\sigma_c}{e^2} = \frac{\sigma_s}{(\hbar/2)^2}$ . (In general, self duality allows another term in the response action :  $\frac{i\theta}{\pi} A \cdot \nabla \times A^S$ ,

i.e., a spin Hall term. However this is forbidden by particle hole symmetry  $PH: A \rightarrow -A$ .) Therefore we expect the critical gauge action to have the following form:

---


$$\mathcal{L}_{eff} = \frac{\sigma_0}{2} \left[ (\nabla \times eA)_\mu \frac{1}{\sqrt{\nabla^2}} (\nabla \times eA)_\mu + (\nabla \times \frac{\hbar}{2} A^S)_\mu \frac{1}{\sqrt{\nabla^2}} (\nabla \times \frac{\hbar}{2} A^S)_\mu \right]. \quad (18)$$


---

Note, in a regular Fermi liquid, a Wiedemann-Franz like relation connects the metallic spin and charge conductivity in precisely the same way, since at low temperatures both quantities are transported by electronic quasiparticles with a fixed charge to spin ratio. At the critical point described above, although we have spin-charge separated excitations, the self duality of the theory restores this Wiedemann-Franz like relation between the metallic spin and charge conductivities.

At criticality the correlations of the magnetic order parameter  $\langle S^+(r, t) S^-(0, 0) \rangle \sim \frac{(-1)^r}{r^2 - c^2 t^2}^{1/2 + \eta/2}$  and the Cooper pair order parameter  $\langle \Delta^*(r, t) \Delta(0, 0) \rangle \sim \frac{1}{r^2 - c^2 t^2}^{1/2 + \eta/2}$  are related by the self duality, and constrained to fall off with the same power law. Since these are both expressed as bilinears of vortex operators, the  $\eta$  exponent is expected to be large. Thus, the critical point unites the antiferromagnetism and superconductivity in a remarkable symmetric fashion.

## V. SLAVE BOSON FORMULATION

In Sec.I we started from a lattice Hamiltonian for a superconductor and showed that the vortices carry spin. We then condensed these vortices and showed that, as a result, the system becomes an AF ordered Mott insulator. In this section we begin with a lattice theory for this Mott insulator, and show that we can arrive at the same conclusions from this different angle. The slave boson gauge theory approach used below, captures both the superconducting and antiferromagnetic insulator phases within a single formulation. While the former is obtained by the Higgs mechanism, the latter, surprisingly, is the Coulomb phase of the gauge theory. This is an interesting counterexample to the standard folklore that slave boson theory can readily describe superconducting states but not magnetically ordered phases. Here we establish that magnetic order of the easy plane variety can indeed be captured.

### A. Insulating State

Consider a half filled strongly correlated electronic model on square lattice.

$$H_{\text{Hubbard}} = H_{\text{hop}} + U \sum_i (n_i - 1)^2 \quad (19)$$

where the first term is a hopping Hamiltonian, while the interaction term tends to prefer single occupancy per site ( $n_i$  is the electron number on site  $i$ ). Unlike most other such models which exhibit spin  $SU(2)$  symmetry we assume that there is only  $S_z$  spin rotation symmetry; this is incorporated in  $H_{\text{hop}}$  via e.g. spin dependent hopping terms.

Deep in the Mott insulating state, when we turn up the value of  $U$ , the physics is described by a spin 1/2 Hamiltonian. For concreteness we consider obtaining the following simple Hamiltonian:

$$H = J \sum_{\langle rr' \rangle} \vec{S}_r \cdot \vec{S}_{r'} + H_{\text{anis}} \quad (20)$$

$$H_{\text{anis}} = -\frac{J_2}{2} \sum_{\langle\langle rr'' \rangle\rangle} (S_r^+ S_{r''}^- + S_r^- S_{r''}^+), \quad (21)$$

where the  $SU(2)$  breaking term comes in as a ferromagnetic second neighbor interaction between planar components of the spin. The ground state of this Hamiltonian is expected to be an easy-plane Neel ordered state with spins in the XY plane.

Below we will show that the same conclusion can be reached via the slave boson formulation in a controllable fashion. This new mechanism for obtaining magnetically ordered states in the slave boson approach is not just of academic interest. It allows us to simultaneously capture the magnetically ordered states and superconductivity (the latter is readily realized using slave bosons as the Higgs particle) within the same formulation. This is achieved without having to resort to 'confinement' which in the slave boson context does not allow for a unique identification of the ordered state. In contrast, the approach presented here will allow us to identify both the XY antiferromagnet and the superconducting phases uniquely. Moreover unifying these two phases within a single formulation leads to the possibility of a direct continuous transition between these two phases. The slave

boson approach also allow us to identify the nature of the superconducting state and the symmetries required to accomplish such a transition.

Consider treating the Hamiltonian (20) using a 'Schwinger fermion' representation of spins, i.e. introduce two component fermions ( $f_{r\uparrow}$ ,  $f_{r\downarrow}$ ) at each site with the constraint:

$$\sum_{\sigma} f_{r\sigma}^{\dagger} f_{r\sigma} = 1 \quad (22)$$

imposed on every site. Then, the spin 1/2 operators are  $\vec{S}_r = \frac{1}{2} f_{r\sigma}^{\dagger} \vec{\sigma}_{\sigma, \sigma'} f_{r\sigma'}$ . Substituting this in (20) leads to a Hamiltonian quartic in the fermionic operators. To make progress, consider the mean field approximation<sup>18,26,27</sup>, obtained by replacing  $\langle f_{r\sigma}^{\dagger} f_{r'\sigma'} \rangle = \chi_{rr', \sigma, \sigma'}$  and treating the constraint on average. It is well known that in the absence of the spin anisotropy term, the optimal mean field ansatz with uniform amplitude is the staggered flux state

$$H_{MF}^{SF} = - \sum_{\langle rr' \rangle} \chi_{rr'} f_{r\sigma}^{\dagger} f_{r'\sigma} \quad (23)$$

with the nearest neighbor hopping amplitudes  $\chi_{rr'} = |\chi| e^{\pm i\Phi/4}$  along (against) the directions shown in the Figure 1(a). The optimal variational state within this set is reached for  $\Phi \approx 0.34\pi$ .<sup>28</sup>

Now let us try to minimize the mean-field energy due to the spin anisotropy term

$$\langle H_{anis} \rangle = \frac{J_2}{2} \sum_{\langle\langle rr'' \rangle\rangle} \langle f_{r\uparrow}^{\dagger} f_{r''\uparrow} \rangle \langle f_{r''\downarrow}^{\dagger} f_{r\downarrow} \rangle. \quad (24)$$

One way in which this can be achieved is if the two expectation values are real but with opposite signs, i.e.

$$H_{MF} = - \sum_{\langle rr' \rangle} \chi_{rr'} f_{r\sigma}^{\dagger} f_{r'\sigma} - \sum_{\langle\langle rr'' \rangle\rangle} \sigma t_{rr''}^s f_{r\sigma}^{\dagger} f_{r''\sigma} \quad (25)$$

the spatial structure of the spin dependent next-neighbor hopping  $t_{rr''}^s$  is shown in the figure 1(a). This choice of  $t_{rr''}^s$  opens a gap at the Dirac points and hence leads to a better mean field energy.

The mean field Hamiltonian above has a familiar form. In the absence of spin dependence of the next neighbor hopping, this is the "chiral spin liquid" Hamiltonian<sup>20</sup>. The spin dependence leads to opposite Chern numbers<sup>21</sup> ( $\pm 1$ ) for the spin up and spin down fermions, and hence describes a spin Hall insulator. However, unlike the honeycomb lattice spin hall insulator introduced in Ref.<sup>22</sup>, this band structure breaks time reversal symmetry, although time reversal invariance combined with a translation is still a symmetry. Note also, that the unit cell is doubled once these spin dependent hoppings are introduced (the staggered flux mean field theory in contrast, is effectively a translationally symmetric ansatz).

## Gauge fluctuations and Neel order

The U(1) symmetry, corresponding to the conservation of the  $f$  fermion number, of Eq. (25) is not a physical symmetry, but rather corresponds to a U(1) gauge redundancy. Including the corresponding gauge field  $a_{rr'}$  on bonds of the lattice, requires  $\chi_{rr'} \rightarrow \chi_{rr'} e^{ia_{rr'}}$  and  $t_{rr''}^s \rightarrow t_{rr''}^s e^{ia_{rr''}}$ . The temporal component of the gauge field  $a_0$  arises as the Lagrange multiplier imposing the constraint (22).

Since the fermions are gapped, they can be safely integrated out to obtain an effective action for the gauge degrees of freedom. In order to interpret this action it is useful to introduce an external 'spin' gauge field  $A_{rr'}^S$ . This is possible since  $S_z$  is a conserved spin density. Replacing  $a_{rr'} \rightarrow a_{rr'} + \frac{\hbar}{2} A_{rr'}^S \sigma^z$ , and integrating out the fermions, one obtains the Euclidean Lagrangian:

$$\mathcal{L}_E[a, A^S] = i \frac{\hbar}{2\pi} A^S \cdot \nabla \times a + \frac{K}{2} [(\nabla \times a)^2 + (\nabla \times \frac{\hbar}{2} A^S)^2] \quad (26)$$

where we have used a three vector notation  $\nabla = (\partial_0, \Delta_x, \Delta_y)$  etc., with lattice derivatives in the space direction. Note, there is no charge Chern Simons term since the net Chern number vanishes. The first term arises because of the opposite Chern numbers for the two spin bands. It associates a spin of  $\hbar/2$  with the  $2\pi$  flux of  $a$ . Finally, the dynamical gauge field ( $a$ ) is non-compact, i.e. there are no monopole configurations created by the dynamics, since a monopole event (which inserts  $2\pi$  flux) is associated with a spin flip, which is forbidden by  $S_z$  conservation. We now integrate out the dynamical gauge field  $a$  to obtain:

$$\mathcal{L}_E[A_{\perp}^S] = \frac{\hbar^2}{32\pi^2 K} [A_{\perp}^S]^2 + \frac{K}{2} [(\nabla \times \frac{\hbar}{2} A^S)^2] \quad (27)$$

the first term is a London term that indicates the phase is a 'spin superfluid'. This implies XY magnetic order, although it does not specify the precise pattern of ordering (i.e. ferromagnetic, vs various Neel ordered states). However, given that the mean field theory is favored by the microscopic Hamiltonian Eq. (20), it is natural to expect this to be the usual Neel ordered state with opposite moments on the two sublattices. Note, since we have already doubled the unit cell, the Neel order is at  $\mathbf{q} = (0, 0)$ , but transforms nontrivially under the point group.

The nature of the order may be established more rigorously as follows. Note, due to the absence of monopole events in the dynamics, one is left with a Maxwell action for the dynamical gauge field  $a$ . The gapless photon excitations that this implies, corresponds to oscillations of the dynamical magnetic flux. However, due to the binding of flux to spin density, this implies a fluctuating  $S_z$  density. In fact, this gapless photon is simply the Goldstone mode associated with XY spin symmetry breaking (see the discussions in section IV). In order to establish the spin order one needs to evaluate  $\langle S_r^+ S_0^- \rangle$ . This corresponds to evaluating the correlators



of the monopole insertion operator  $\langle V_r^\dagger V_0 \rangle$ . It is well known<sup>29</sup>, that in magnetically Coulomb phase in  $D=2$ , the monopole operators have long range order. The precise ordering pattern corresponds to the transformation properties of the monopole insertion operator under the lattice symmetries. This is explicitly evaluated in Appendix F where it is confirmed that we indeed obtain the Neel state. Note, this phase is entirely identical to the regular XY Neel ordered state, although it is obtained from such an 'exotic' starting point. The magnetic order induced by gauge fluctuations ensures, for example, that the counter-propagating edge states implied by the mean field theory are gapped.

## B. Charge Fluctuations

Consider lowering the charge gap to approach the Mott transition so that the electron occupation at each site can now fluctuate into the  $n = 0$  and  $n = 2$  state as well. This is achieved by lowering the value of  $U$  in equation 19. These fluctuations are typically incorporated via the slave rotor formulation<sup>30,31</sup>, by introducing a rotor variable  $z_r = e^{i\phi_r}$  and its conjugate number variable  $N_r$  at each site. The electron operator is then written as  $c_{r\sigma}^\dagger = z_r f_{r\sigma}^\dagger$ , and the constraint now reads  $n_r^f + N_r = 1$ . This however does not capture all Mott transitions, for example it was pointed out that Hubbard models with pseudospin symmetry requires introducing a  $SU(2)$  slave rotor<sup>32</sup> which is a simple extension of the  $SU(2)$  slave boson theory<sup>33</sup> to include both electron and hole fluctuations. A pair of complex fields  $z_{1r}, z_{2r}$  are introduced, which are  $SU(2)$  'rotor' variables i.e.  $|z_{1r}|^2 + |z_{2r}|^2 = 1$ . The electron operator is written as:

$$\begin{aligned} c_{r\uparrow} &= f_{r\uparrow} z_{r1} - \eta_r f_{r\downarrow}^\dagger z_{r2}^\dagger \\ c_{r\downarrow} &= f_{r\downarrow} z_{r1} + \eta_r f_{r\uparrow}^\dagger z_{r2}^\dagger. \end{aligned} \quad (28)$$

if we define:

$$\Psi_r = \begin{bmatrix} c_{r\uparrow} \\ \eta_r c_{r\downarrow}^\dagger \end{bmatrix} \quad F_r = \begin{bmatrix} f_{r\uparrow} \\ \eta_r f_{r\downarrow}^\dagger \end{bmatrix} \quad (29)$$

$$Z_r = \begin{pmatrix} z_{i1} & -z_{i2}^\dagger \\ z_{i2} & z_{i1}^\dagger \end{pmatrix} \quad (30)$$

$$\Psi_r = Z_r F_r \quad (31)$$

the electron operator may be written compactly as in the last line; where  $Z_r$  is an  $SU(2)$  matrix. The mean field Hamiltonian (25) takes on a particularly simple form in this notation:

$$H_{MF} = \sum_{rr'} F_r^\dagger (\chi_{rr'}^R + t_{rr'}^s + i\chi_{rr'}^I \mu_z) F_{r'} \quad (32)$$

with  $\chi_{rr'} = \chi_{rr'}^R + i\chi_{rr'}^I$  and with diagonal spin dependent hoppings  $t_{rr'}^s$  as shown.

This definition has an  $SU(2)$  redundancy, clearly any set of  $SU(2)$  matrices  $U_r$  can generate the transformation  $Z_r \rightarrow Z_r U_r^\dagger$ ,  $F_r \rightarrow U_r F_r$  leaving the form above

invariant. Naturally, there is a close connection between this redundancy and the constraint that needs to be implemented to obtain the physical Hilbert space. If the operators  $\mathbf{T}_r$  generates the above transformations, then the constraint on physical states is that  $\mathbf{T}_r = 0$ .

Luckily for our purposes we will not need the full  $SU(2)$  formulation. Instead, we only retain the fact that there are a doublet of charged bosons, but assume that they are rotor variables with equal amplitude  $z_{1r} = \frac{1}{\sqrt{2}} e^{i\phi_{1r}}$ ,  $z_{2r} = \frac{1}{\sqrt{2}} e^{i\phi_{2r}}$ . This form is necessary, and sufficient, to incorporate the gauge fluctuations and symmetries of the mean field theory Eq. (25). The  $SU(2)$  matrices  $U$  that preserve this structure are generated by  $U_\epsilon = e^{i\epsilon\mu_z}$ , and  $U^I = i\mu_x$  where  $\mu$  are  $2 \times 2$  Pauli matrices in the usual representation. While the former is simply the  $U(1)$  gauge transformation that leaves the mean field Hamiltonian invariant, the latter appears as the gauge transformation required to implement reflection symmetry (Appendix C). Hence, in the absence of a two component slave rotor theory, we would be unable to implement this physical symmetry starting with the mean field theory Eq. (25). If we now define  $N_{1r}$  and  $N_{2r}$  as the operators conjugate to the two phase variables, the physical states in the basis  $|N_1, N_2; n_f^\uparrow, n_f^\downarrow\rangle$  satisfy the constraints  $(N_1 + N_2) + (n_f^\uparrow + n_f^\downarrow) = 1$  and invariance under the combination of  $|N_1, N_2\rangle \rightarrow (-1)^{N_1} |N_2, -N_1\rangle$  and  $|n_f\rangle \rightarrow \eta_r (f_{r\uparrow}^\dagger f_{r\downarrow} + f_{r\downarrow}^\dagger f_{r\uparrow}) |n_f\rangle$ . This constrains the physical states on a site to be:

$$|\uparrow\rangle = |0, 0; \uparrow\rangle \quad (33)$$

$$|\downarrow\rangle = |0, 0; \downarrow\rangle \quad (34)$$

$$|0\rangle = (|0, 1; \rangle + \eta_r |1, 0; \uparrow\downarrow\rangle) \quad (35)$$

$$|\uparrow\downarrow\rangle = (-\eta_r |1, 0; \rangle + |0, -1; \uparrow\downarrow\rangle) \quad (36)$$

A physical interpretation of the charge boson doublet is provided at the end of appendix G 3.

## The superconducting phase

An advantage of the two component slave rotor formulation above is that the superconducting state is very naturally described. As the Mott transition is approached, the gap to the charge excitations closes, at which point  $z_1, z_2$  condense. If both bosons condense individually,  $\langle z_1 \rangle = \Phi_1$ ,  $\langle z_2 \rangle = \Phi_2$  a superconductor is obtained. This can be verified by noting that the gauge invariant quantity  $\langle z_1^\dagger z_2 \rangle = \Phi_1^* \Phi_2$  which is the superconducting order parameter, has long range order.

Once the charged bosons are condensed, the electron  $\Psi_r$  has a finite overlap with the 'spinon'  $F_{r\sigma}$ , and inherits its dispersion. Since  $\Psi_r \sim \langle Z \rangle F_r$ , and  $\langle Z \rangle = \sqrt{|\Phi_1|^2 + |\Phi_2|^2} U_\Phi$ , where  $U_\Phi$  is a unitary matrix, an effective Hamiltonian that describes the electron excitation can be readily obtained from the mean field Hamiltonian (32):

$$H_e = \sum_{rr'} \Psi_r^\dagger U_\Phi (\chi_{rr'}^R + t_{rr'}^s + i\chi_{rr'}^I \mu_z) U_\Phi^\dagger \Psi_{r'} \quad (37)$$

when both bosons are condensed with equal magnitude  $\Phi_1 = e^{i\theta}\Phi_2$ , the electronic Hamiltonian is just:

$$H_{dSc} = \sum_{rr'} c_{r\sigma}^\dagger (\chi_{rr'}^R + t_{rr'}^s) c_{r'\sigma'} + \Delta_{rr'} \epsilon_{\sigma\sigma'} c_{r\sigma}^\dagger c_{r'\sigma'}^\dagger + \text{h.c.} \quad (38)$$

where the pairing function  $\Delta_{rr'} = ie^{i\theta}\eta_{r'}\chi_{rr'}^I$  is symmetric upon  $r \leftrightarrow r'$  and changes sign under  $\pi/2$  rotation. Hence it is a spin singlet d-wave pairing function. If  $t^s = 0$  this is the regular  $d_{x^2-y^2}$  superconductor with translation symmetry and nodes at  $(\pm\pi/2, \pm\pi/2)$ . The addition of the spin dependent hopping opens a gap at these nodes. It doubles the unit cell and breaks time reversal symmetry (although the combination of a unit translation and time reversal remains a symmetry). Note however, since the above SC Hamiltonian is a unitary transformation of the hopping Hamiltonian  $H_{MF}$ , it shares the same spectrum. In particular, since the hopping Hamiltonian had a nontrivial band structure and was argued to have counter-propagating spin filtered edge modes. The same is true of the superconducting Hamiltonian above. However, once the charge bosons condense, additional terms are allowed in the fermion Hamiltonian, which are forbidden in the insulating state. For example, one can add terms corresponding to ‘spinon pairing’, which are forbidden by the gauge U(1) symmetry on the insulating state. Such terms can arise simply from the electron’s next neighbor hopping, which in the two component notation corresponds to  $\psi_r^\dagger \mu^z \psi_{r'} = F_r^\dagger Z^\dagger \mu^z Z F_r = |\Phi|^2 F_r^\dagger \mu^x F_r$ . Note however, the strength of such a term is proportional to the condensate density, and becomes very small near the transition. Including these terms removes the nontrivial topological properties (such as gapless edge states) of the superconductor. Therefore, the superconducting state obtained on boson condensation is a generic d-wave superconductor with doubled unit cell. If, however, we demand particle hole symmetry, then terms like the second neighbor hopping term above are forbidden, and the superconductor indeed has nontrivial band topology (see appendix G 2). In our previous analysis it was convenient to consider a particle hole symmetric superconductor, although it is difficult to demand that as the microscopic symmetry of a physical system. Luckily, we show in Sec.VII that demanding complete particle hole symmetry is unnecessary - instead we need only tune one chemical potential type term to zero, to obtain a direct relativistic transition.

We note in passing that condensing just one of the two  $(z_1, z_2)$  fields leads to a topological band insulator (TBI). (At the end of Sec.V C we show that these states are realized in the SC vortex core.) In choosing one of these fields to condense, one spontaneously breaks the reflection symmetry. If  $z_1$  condenses, the appropriate mean-field electronic Hamiltonian can be obtained from Eq. (25) by replacing  $f_\sigma \rightarrow c_\sigma$ . Similarly if  $z_2$  condenses we simply make a different replacement:  $f_\sigma \rightarrow \eta_r \epsilon_{\sigma\sigma'} c_{\sigma'}^\dagger$ . The above different condensation scenario of  $z_1$  and  $z_2$  can be summarized by the vector  $\vec{n} = z^\dagger \vec{\sigma} z$  where  $z = (z_1, z_2)$ .

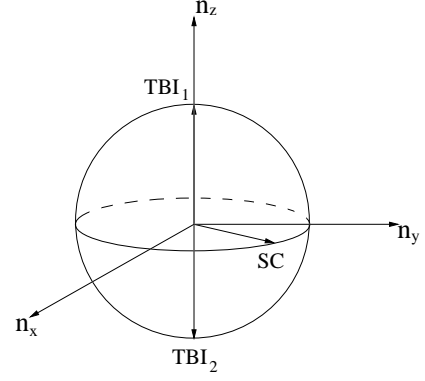


FIG. 6: The  $\vec{n}$  sphere and the corresponding electronic phases.

Using  $\vec{n}$  we represent the topological insulator (TBI) associated with  $\langle z_1 \rangle \neq 0$  and  $\langle z_2 \rangle = 0$  (TBI<sub>1</sub>) by  $\vec{n}$  pointing to the north pole. Similarly the TBI associated with  $\langle z_1 \rangle = 0$  and  $\langle z_2 \rangle \neq 0$  (TBI<sub>2</sub>) by  $\vec{n}$  pointing to the south pole. The particle hole transformation transform TBI<sub>1</sub> into TBI<sub>2</sub> and vice versa. The d-wave SC discussed throughout the early part of the paper is represented by  $\vec{n}$  lying in the xy plane. This is illustrated in Fig.(6).

### C. The field theory of transition

Consider approaching the transition from the insulating state. The charged bosons are gapped but acquire a dispersion from the electron hopping Hamiltonian 19. This includes the regular nearest neighbor hopping  $H_{\text{hop}}^{\text{NN}} = -t \sum_{\langle rr' \rangle} c_{r\sigma}^\dagger c_{r'\sigma'}$ , which we treat in detail below (other hopping terms lead to similar results). Expanding the electron operator as in Eq. (28), and assigning the mean field expectation values to the spinon bilinears  $J(\sum_\sigma f_{r\sigma}^\dagger f_{r'\sigma}) = \chi_{rr'}$ , one also obtains a staggered flux dispersion for the  $z$ -bosons:  $H_{\text{hop}} = -\frac{t}{j} \sum \chi_{r'r} (z_{1r}^\dagger z_{1r'} + z_{2r}^\dagger z_{2r'})$ . This dispersion has a unique minimum (for flux  $\Phi \neq \pi$ ) which is relevant to the low energy theory.

The low energy field theory of the transition is argued below to take the following form:

$$\begin{aligned} \mathcal{L}_E &= \mathcal{L}^z + \mathcal{L}^f & (39) \\ \mathcal{L}_f &= i \frac{\hbar}{2\pi} A^S \cdot \nabla \times a \\ \mathcal{L}^z &= \sum_{\mu, \alpha} |(\partial_\mu - ia_\mu) z_\alpha|^2 + \frac{K}{2} (\nabla \times a)^2 + V + \Delta \mathcal{L} \\ V &= r(|z_1|^2 + |z_2|^2) + U(|z_1|^2 + |z_2|^2)^2 - \lambda |z_1|^2 |z_2|^2 \\ \Delta \mathcal{L} &= \mu [z_1^* (\partial_\tau - ia_0) z_1 - z_2^* (\partial_\tau - ia_0) z_2] \end{aligned}$$

The Euclidean Lagrangian consists of two pieces, one arising from integrating out the fermionic spinons  $\mathcal{L}_f$  and one for the  $z$ -bosons  $\mathcal{L}^z$ , coupled to an low-energy U(1) fluctuating gauge field  $a$ . Note, the representation of the electron operator in Eq. 31 implies that the  $z$ -bosons are also minimally coupled to the U(1) gauge field of the

spinons. The remaining terms appearing in  $\mathcal{L}^z$  are the ones allowed by the symmetries of the problem, which act on these bosons in a nontrivial manner as described in Appendix C. Since the fermionic spinons are gapped throughout the transition, they can be safely integrated out. This produces the spin Hall effective action  $\mathcal{L}_f$  since the mean-field state of the spinon is a spin hall insulator. (Note that to the spinons  $a$  plays the role of the charge gauge field.) Symmetries prohibit other terms in this low energy action. For example, (see appendix C ) under reflections about the x or y axis passing through a plaquette center, the fields transform according to  $z_1 \rightarrow z_2^*$ ,  $z_2 \rightarrow -z_1^*$ , in addition to the reflection of coordinates. This symmetry rules out terms like  $|z_1|^2 - |z_2|^2$  and  $z_1^* \partial_\tau z_1 + z_2^* \partial_\tau z_2$ . It does however allow the linear time derivative term  $\Delta\mathcal{L}$ . While point group symmetries do not forbid a background flux term like  $h(\partial_x a_y - \partial_y a_x)$ , taking into account symmetry under time reversal (followed by translation) rules out such a term. (Only a staggered background flux is allowed, but this has already been incorporated while deriving the  $z$ -boson dispersion.)

In the absence of  $\Delta\mathcal{L}$ , the effective action for the transition is in the easy-plane NCCP<sub>1</sub> universality class<sup>9</sup>. As we discussed at the beginning of the paper, the nature of direct transition (whether it is generically fluctuation driven first order) in the relativistic easy-plane NCCP<sub>1</sub> model is controversial. In contrast, in the presence of  $\Delta\mathcal{L}$  the non-relativistic NCCP<sub>1</sub> transition in  $d+z=4$  has been studied using perturbative RG<sup>34</sup>. The conclusion is that fluctuation generically drives the transition to first order.

In order to access the relativistic transition, one needs to tune both  $r$  and  $\mu$  to zero in equation (39). The latter corresponds to a chemical potential since  $z_1$  and  $z_2$  carry opposite electrical charge. *It is important that one only need to tune two parameters to reach the relativistic critical point. Because it implies this critical point is realizable in a two dimensional phase diagram.* Physically  $\mu$  measures the deviation from half-filling. In the AF insulator phase the charge density remains fixed for a range of  $\mu$ , due to the charge incompressibility. In the SC phase the charge density does change with chemical potential and one would need to fine tune  $\mu$  to reach the relativistic NCCP<sub>1</sub> quantum critical point.

The above situation is analogous to the simpler case of accessing the relativistic XY transition in the superfluid-Mott insulator transition of the Bose Hubbard model<sup>35</sup>. There, the relativistic transition occurs at the tip of the superfluid lobe, while moving away from this point leads to a non-relativistic Bose Einstein condensation transition with dynamical critical exponent  $z=2$ . In Fig.(7) we present an analogous (schematic) phase diagram in the plane spanned by the chemical potential  $\mu$  and interaction strength  $U$ .

As being discussed in Sec.V A, the electromagnetic field associated with the gauge field  $a$  corresponds to the 3-current of  $S_z$  arising from the gaussian fluctua-

tion in the magnetic XY order. Since  $z_1$  and  $z_2$  couple to  $a$  as charges, it is natural to associated them with the magnetic vortices. From the earlier discussions we see that they carry electrical charge. A related observation is that in the superconducting state near the critical point, the superconducting vortices carry spin. This can be seen as follows. Consider an equal amplitude condensate  $\langle z_1 \rangle = \sqrt{\rho} e^{i\phi_1}$ ,  $\langle z_2 \rangle = \sqrt{\rho} e^{i\phi_2}$ . The energy cost of a static vortex is then obtained from the lagrangian above as  $E = \rho(\nabla\phi_1 - a - eA/\hbar)^2 + \rho(\nabla\phi_2 - a + eA/\hbar)^2$ , where  $A$  is the external vector potential that induces vorticity. A unit vortex with  $\oint A \cdot dl = h/2e$  can be created either with (1)  $\oint \nabla\phi_1 \cdot dl = 2\pi$ ,  $\oint \nabla\phi_2 \cdot dl = 0$  and  $\oint a \cdot dl = \pi$  or with (2)  $\oint \nabla\phi_1 \cdot dl = 0$ ,  $\oint \nabla\phi_2 \cdot dl = 2\pi$  and  $\oint a \cdot dl = -\pi$ . Due to the presence of  $\mathcal{L}_f$  which attaches spin to emergent flux, these vortices carry spin  $\pm\hbar/2$ . Thus, near the transition, the low energy vortices in the antiferromagnet carry charge  $\pm e$  while vortices in the superconductor carry spin  $\pm\hbar/2$ . Thus, a direct transition between these phases can be explained on the basis of the condensation of these defects.

Finally before closing this section we note that the mechanism that generates magnetic order studied here does not require ‘‘confinement’’ which is invoked in other slave boson theories. The advantage of our mechanism is that it allows us to identify both the nature of the magnetic order, which has not been possible in confinement type approach, and the superconducting pairing symmetry unambiguously.

## VI. ROAD MAP TO THE APPENDICES

Before concluding, we outline the content of a number of appendices. They are presented either to elaborate points made in the text, or because they are interesting digression which contribute to the general understanding of subjects covered by this paper. Appendix A contains the technical details of the duality transformation. Such transformation allows one to go back and forth between Eq. (9) and Eq. (13). Appendix B contains the Bogoliubov deGennes treatment of the core state of superconducting vortices. It compliments our numerical results presented earlier. Appendix D present a mean-field theory for the XY ordered state and study the core states of the AF vortices. Appendix E provides details of the vortex tunneling amplitude calculation in both the SC and the AF phases, where we explicitly compute the XY order pattern (AF) from the SC vortex tunneling, and the SC pairing symmetry (d-wave) from the AF vortex tunneling. Appendix C is devoted to the symmetry analysis of the slave boson theory in the AF phase and the transformation properties of the antiferromagnetic vortices. Appendix F presents the quantum number of the monopole operator of Eq. (16) within the slave rotor theory. Appendix G gathers some miscellaneous discussions mentioned in the main text. Finally Appendix H discusses the direct transition between an f-wave SC and

AF magnetic phase on the honeycomb lattice, which is a direct application of the techniques that we learned in the current square lattice case.

## VII. CONCLUSION

In this paper we present a theory exhibiting a d-wave superconductor and an easy-plane antiferromagnetic insulator as its two phases. Unlike ordinary d-wave superconductor, our superconductor has a full gap due to nodes mixing caused by a translation symmetry breaking. In addition, the topological defects, namely vortices, of each of these phases carry the quantum number of the order parameter for the other phase. We derived the effective field theory describing the superconductor to AF insulator phase transition. It is the easy-plane non-compact  $CP_1$  model. The possible phase transition scenarios of this model, include: (1) a direct continuous SC-AF transition, (2) a direct first order SC-AF phase transition, and (3) two consecutive continuous transitions linking SC to a SC+AF coexistence phase and finally to AF. In particular, if scenario (1) is realized, it would constitute an realization of Landau forbidden transition. While the first two scenarios correspond to the condensation of the fundamental vortices in theory, the third requires the condensation of a composite of the fundamental vortices.

Physically this phase transition requires tuning the interaction strength (or the bandwidth) at fixed, half, filling factor. We specified the symmetry requirements for its existence. When the filling factor deviates from  $1/2$  the transition generically becomes first order. In Fig.7 we present a schematic phase diagram in the interaction strength - chemical potential plane. For a range of chemical potential where the superconductor remains fully gapped with the minimum gap (left panel of Fig.8) occurring at  $(\pm\pi/2, \pm\pi/2)$  in the square lattice Brillouin zone. For sufficiently large chemical potential deviation (from that of half filling) the superconducting gap closes. When that happens the quasiparticle spectrum becomes that of a conventional  $d_{x^2-y^2}$  superconductor (right panel of Fig.8), and the positions of the node change with chemical potential.

In the above discussion we have assumed that upon doping the AF-SC transition is direct. It is also possible that such transition proceeds in an indirect manner. For example, imagine a situation the doped charge in the AF insulator are accommodated as charged vortices  $z_1$  and  $z_2$ . To minimize the cost in kinetic energy, it is favorable to keep the total vorticity zero, so that there are equal number of vortex and antivortex. Thus, if the doping is n-type, there will be an equal number of  $z_1$  and  $z_2^\dagger$  vortices (recall that  $z_1$  and  $z_2$  vortex carry opposite charge), while for p-type doping there will be the same number of  $z_2$  and  $z_1^\dagger$  vortices. Due to the logarithmic attraction, it is energetically favorable for  $z_1, z_2^\dagger$  or  $z_1^\dagger, z_2$  to form charge  $\pm 2e$  bound pairs. Because these pairs carry no

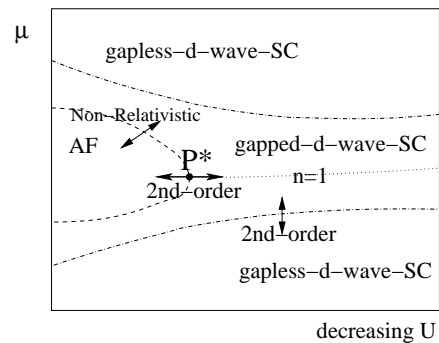


FIG. 7: The schematic global phase diagram. The horizontal axis is the interaction strength,  $U$ , and the vertical axis is the chemical potential  $\mu$ . The dashed lines mark the non-relativistic phase transition at mean-field level (which is likely to be first-order beyond mean-field theory). This transition line terminates at the  $PH$  symmetric critical point  $P^*$  discussed in the present work. Along the dotted line the average charge density is  $\langle n \rangle = 1$ , i.e., half-filling. The SC phase surround the the AF phase is a fully gapped d-wave superconductor. Upon changing of chemical potential the quasiparticle gap closes and the SC undergoes a second-order Lifshitz transition into the nodal gapless d-wave SC at the dash-dotted lines. The quasiparticle spectrum of the gapless d-wave superconductor is identical to that seen in high  $T_c$  superconductors.

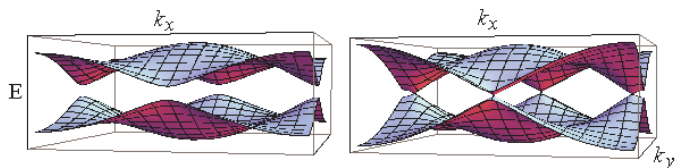


FIG. 8: In the presence of a sufficiently large chemical potential  $\mu$  the nodes of a conventional d-wave superconductor is restored. The parameters used in this figure are  $\phi = \pi/5, t = 0.2$  and left panel  $\mu = 0$ , right panel  $\mu = 0.5$ .

net vorticity, their condensation does not destroy the AF order. Hence a SC and AF coexistence phase emerge. Such a transition is of the usual non-relativistic XY universality. In the coexistence phase, due to the non-zero  $\langle z_2^\dagger z_1 \rangle$  or  $\langle z_1^\dagger z_2 \rangle$ , the  $z_1$  and  $z_2$  AF vortices mixes, and as the result only one AF vortex  $\tilde{z} = \alpha z_1 + \beta z_2$  (where  $\alpha, \beta$  are complex mixing coefficient) is left as low energy excitations. When  $\tilde{z}$  condenses the AF order is finally destroyed and the system becomes a pure superconductor. The coexistence  $\rightarrow$  AF transition is also of the usual XY universality class.

It is also interesting to look at the indirect transition from the superconducting side. As discussed at the beginning, such transition is triggered by the condensation of the composite vortex  $\Psi_\uparrow^\dagger \Psi_\downarrow$ . Such composite vortex carries spin quantum number 1 but no net vorticity (of the superconducting order parameter). As the SC to SC+AF coexistence transition is approached, this excita-

tion will become the lowest-energy magnetic excitation. Like the roton in a superfluid, such vortex-antivortex pair will carry a finite momentum. Such momentum will shift the momentum of the minimum energy  $\Psi_{\uparrow}^{\dagger}\Psi_{\downarrow}$  away from  $(\pi, \pi)$ , similar to the incommensurate magnetic excitation of the high  $T_c$  compounds.

We note that the similar ideas that the defects in the AF phase can carry charge and the defects in the SC phase can carry spin, are introduced in the phase string theory<sup>10,11,12</sup> in the context of High- $T_c$  superconductor. Although there are some significant differences between the current work and the phase string theory: for example, we require the doubling of unit cell, easy-plane spin anisotropy and full energy gap on both AF and SC phases, it is still possible that there are underlying relations which are left for future investigations.

The above discussions are intended to point out some similarity of the phenomenology in our model and that of the cuprate superconductors. However, due to the symmetry difference in the superconducting state, the connection is by no means clear. Nonetheless it is interesting to explore the possible relation with the cuprates in future studies.

This work is supported by nsf-dmr 0645691, LBNL DOE-504108 and DOE DE-AC02-05CH11231.

## APPENDIX A: DUALITY AND SYMMETRIES OF THE SUPERCONDUCTOR VORTEX THEORY

We first fix the relation between the relativistic vortex fields  $\Psi_{\downarrow}$ ,  $\Psi_{\uparrow}$  and the canonical vortex creation and destruction operators. In Eq. (9)

$$\begin{aligned}\Psi_{\uparrow} &= (\psi_{AV\uparrow} + e^{-i\beta}\bar{\psi}_{B\bar{V}\downarrow})/\sqrt{2} \\ \Psi_{\downarrow} &= (\psi_{BV\downarrow} + e^{-i\beta}\bar{\psi}_{A\bar{V}\uparrow})/\sqrt{2},\end{aligned}\quad (\text{A1})$$

where  $\psi_{AV\uparrow}$  bosonic vortex field for the  $AV\uparrow$  vortices, and etc (For more discussions see the end of this paragraph). The phase  $\beta$  is the phase of the annihilation matrix elements of  $(AV\uparrow, B\bar{V}\downarrow)$  and  $(BV\downarrow, A\bar{V}\uparrow)$ , respectively (the

reason that these two phase factor are the same is due to the  $T \circ \uparrow \leftrightarrow \downarrow$  symmetry). We note that in terms of  $\Psi_{\uparrow, \downarrow}$  Eq. (9) has a relativistic form. It can be derived from a theory where  $\psi_{AV\uparrow}, \psi_{A\bar{V}\uparrow}, \psi_{BV\downarrow}$  and  $\psi_{B\bar{V}\downarrow}$  are treated as non-relativistic fields; in the presence of pair creation and pair annihilation terms  $-|J|e^{i\beta}\psi_{AV\uparrow}\psi_{B\bar{V}\downarrow} + c.c$  the combination  $(\psi_{AV\uparrow} - e^{-i\beta}\bar{\psi}_{B\bar{V}\downarrow})/\sqrt{2}$  and  $(\psi_{BV\downarrow} - e^{-i\beta}\bar{\psi}_{A\bar{V}\uparrow})/\sqrt{2}$  become the more massive fields and hence can be dropped from the low energy theory. The left low energy combinations is given in Eq. (A1). The important thing is that in the derivation sketched above it is assumed that  $\psi_{AV\uparrow}, \psi_{A\bar{V}\uparrow}, \psi_{BV\downarrow}$  and  $\psi_{B\bar{V}\downarrow}$  are all degenerate with respect to one another (in the sense that permuting any two fields will leave the (non-relativistic) action invariant. This important degeneracy is guaranteed by the symmetry of operations of Eq. (5).

Note that according to Eq.(5)  $PH$  transforms a vortex into an anti-vortex, while preserving spin, while mirror reflection  $\mathcal{P}$  also transforms a vortex into an anti-vortex, while preserving the spin. Finally,  $T \circ \mathcal{TR}$  transforms a vortex into an anti-vortex and flips spin. Thus we have:

$$\begin{aligned}PH: AV\uparrow &\rightarrow A\bar{V}\uparrow & BV\downarrow &\rightarrow B\bar{V}\downarrow, \\ &\Rightarrow \Psi_{\uparrow} \rightarrow \Psi_{\downarrow}^{\dagger} & \Psi_{\downarrow} &\rightarrow \Psi_{\uparrow}^{\dagger}\end{aligned}\quad (\text{A2})$$

$$\begin{aligned}\mathcal{P}: AV\uparrow &\rightarrow A\bar{V}\uparrow & BV\downarrow &\rightarrow B\bar{V}\downarrow, \\ &\Rightarrow \Psi_{i\uparrow} \rightarrow \Psi_{\mathcal{P}(i)\uparrow}^{\dagger} & \Psi_{\downarrow} &\rightarrow \Psi_{\mathcal{P}(i)\uparrow}^{\dagger}\end{aligned}\quad (\text{A3})$$

$$\begin{aligned}T \circ \mathcal{TR}: AV\uparrow &\rightarrow B\bar{V}\downarrow & BV\downarrow &\rightarrow A\bar{V}\uparrow, \\ &\Rightarrow \Psi_{\uparrow} \rightarrow \Psi_{\downarrow}^{\dagger} & \Psi_{\downarrow} &\rightarrow \Psi_{\uparrow}^{\dagger} \text{ (anti-unitary)}\end{aligned}\quad (\text{A4})$$

this allows us to restrict our field theory to the form in equation Eq. (9).

### Duality:

We now carry through the duality starting with Eq. (9). We first set  $\Psi_{\sigma} = \sqrt{\bar{\rho}}\phi_{\sigma}$  at long wavelength/time, where  $\bar{\rho}$  is the average condensate density of the up and down vortices, and  $\phi_{\sigma}$  is a  $U(1)$  phase factor. Subsequently we can introduce auxiliary fields  $J_{\mu}^{\sigma}$  so that

$$e^{\{-\int d^2x dt \sum_{\sigma} \sum_{\mu} |(\partial_{\mu} + i\alpha_{\mu} - i\frac{\hbar}{2}A_{\mu}^S \sigma^3)\Psi_{\sigma}|^2\}} = \int D[J_{\mu}^{\sigma}] e^{\{-\int d^2x dt [\sum_{\mu\sigma} \frac{4}{\bar{\rho}}(J_{\mu}^{\sigma})^2 - J_{\mu}^{\sigma}(\bar{\phi}_{\sigma}\partial_{\mu}\phi_{\sigma} + i\alpha_{\mu} - i\frac{\hbar}{2}A_{\mu}^S)\]}\}} \quad (\text{A5})$$

Next, we separate  $\bar{\phi}_{\sigma}\partial_{\mu}\phi_{\sigma}$  into  $\bar{\phi}_{\sigma}\partial_{\mu}\phi_{\sigma} = i\partial_{\mu}\theta_{\sigma} + \bar{\phi}_{\sigma}^v\partial_{\mu}\phi_{\sigma}^v$ , where  $\bar{\phi}_{\sigma}^v$  denotes the topological non-trivial part (i.e., the vortex containing part) of  $\phi_{\sigma}$ . Integrating out  $\theta_{\sigma}$  generates the constraint  $\partial_{\mu}J_{\mu}^{\sigma} = 0$ . This constraint is

solved via the introduction of two new ‘‘gauge fields’’  $J_{\mu}^{\sigma} = \frac{1}{2\pi}(\nabla \times a^{\sigma})_{\mu}$ . Now we collect all the  $\alpha_{\mu}$  and  $a_{\mu}$  dependent terms in the action to obtain

$$\int d^2x dt \sum_{\sigma\mu} \left\{ \frac{1}{\pi^2 \bar{\rho}} (\nabla \times a^\sigma)_\mu^2 - i a_\mu^\sigma \left[ K_\mu^\sigma + \frac{1}{2\pi} (\nabla \times \alpha)_\mu - \frac{\hbar\sigma}{4\pi} (\nabla \times A^S)_\mu \right] + \frac{\kappa}{2} (\nabla \times a)^2 + i \frac{e}{\pi} A \cdot (\nabla \times \alpha) \right\}. \quad (\text{A6})$$

In Eq. (A6)  $K_\mu^\sigma = -\frac{i}{2\pi} \phi_\sigma^v \partial_\mu \phi_\sigma^v$  is the 3-current of the vortex of superconducting vortices (i.e., the vortex of  $\psi_\sigma$  bosons). Next, we integrate out  $\alpha_\mu$  which leads to

$$\sum_{\sigma} (\nabla \times a^\sigma)_\mu = 2e(\nabla \times A)_\mu + \text{less relevant terms} \\ \text{at long wavelength.} \quad (\text{A7})$$

Eq. (A7) fixes the flux in  $a^\uparrow + a^\downarrow$  and leaves the flux of  $a^\uparrow - a^\downarrow$  free to fluctuate. Let us define  $a_\mu = (a_\mu^\downarrow - a_\mu^\uparrow)/2$ , then the remaining part of Eq. (A6) reduces to

$$S_{\text{dual}} = \int d^2x dt \sum_{\sigma\mu} \left\{ \frac{1}{\pi^2 \bar{\rho}} [e^2 (\nabla \times A)_\mu^2 + (\nabla \times a)_\mu^2] - ie A_\mu (K^\uparrow + K^\downarrow)_\mu + ia_\mu (K^\uparrow - K^\downarrow)_\mu - \frac{i\hbar}{2\pi} (\nabla \times a) \cdot A^S \right\}. \quad (\text{A8})$$

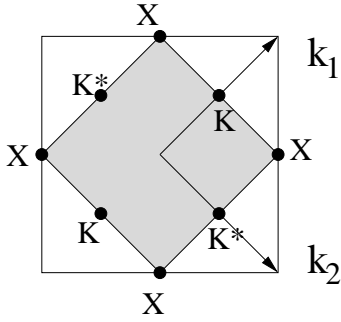


FIG. 9: The reduced Brillouin Zone (shaded area) of the model Eq.(1).

If we identify

$$K_\mu^\uparrow \leftrightarrow \text{the 3-current of } z_1 \text{ boson} \\ -K_\mu^\downarrow \leftrightarrow \text{the 3-current of } z_2 \text{ boson,} \quad (\text{A9})$$

Eq. (A8) can be recognized as the Feynman path integral

representation of the second quantized action in Eq. (13).

## APPENDIX B: BOGOLIUBOV DEGENNES ANALYSIS OF THE SUPERCONDUCTING VORTICES

In section I we have determined the core structure of the superconducting vortices numerically. To make sure that our numerical results are universal, in this section we present an analytical study in the long wavelength limit. Interestingly, as a by-product, we obtain a new situation where zero modes exist in a non-Dirac like Hamiltonian.

We first write down the d-wave pairing Hamiltonian Eq.(1) in the momentum space:

$$H = \sum_k \Psi_k^\dagger H(k) \Psi_k, \quad (\text{B1})$$

where

$$H(k) = \begin{pmatrix} 2t(\cos k_2 - \cos k_1) & \chi_1(1 + e^{-i(k_1+k_2)} + e^{-ik_1} + e^{-ik_2}) & 0 & \chi_2^* (-1 - e^{-i(k_1+k_2)} + e^{-ik_1} + e^{-ik_2}) \\ \chi_1(1 + e^{i(k_1+k_2)} + e^{ik_1} + e^{ik_2}) & -2t(\cos k_2 - \cos k_1) & \chi_2^* (-1 - e^{-i(k_1+k_2)} + e^{-ik_1} + e^{-ik_2}) & 0 \\ 0 & \chi_2(-1 - e^{-i(k_1+k_2)} + e^{-ik_1} + e^{-ik_2}) & 2t(\cos k_2 - \cos k_1) & -\chi_1(1 + e^{-i(k_1+k_2)} + e^{-ik_1} + e^{-ik_2}) \\ \chi_2(-1 - e^{i(k_1+k_2)} + e^{ik_1} + e^{ik_2}) & 0 & -\chi_1(1 + e^{i(k_1+k_2)} + e^{ik_1} + e^{ik_2}) & -2t(\cos k_2 - \cos k_1) \end{pmatrix} \quad (\text{B2})$$

In Eq. (B1) and Eq. (B2)

$$\Psi_k = (c_{A\uparrow k}, c_{B\uparrow k}, c_{A\downarrow -k}^\dagger, c_{B\downarrow -k}^\dagger), \quad (\text{B3})$$

and we denote  $Re(\chi) = \chi_1$  and  $Im(\chi) = \chi_2$ . We allow  $\chi_2$  to be a complex number since the pairing amplitude gain a phase under the charge- $U(1)$  rotation.  $k_1$  and  $k_2$  are

the momentum components along the reduced reciprocal lattice vectors in Fig.(9).

Let us first study the parameter regime:  $|\chi_1| \sim 1$ ,  $|\chi_2| \sim 1$  and  $|t| \ll 1$ . If  $t = 0$  we have a gapless d-wave superconductor with two inequivalent Dirac nodes at  $K$  and  $K^*$  (see Fig.9). The  $t$  term mixes  $K$  and  $K^*$  and opens up a small gap. In this limit we can linearize the Hamiltonian matrix Eq.(B2) around  $K$  as:

$$H_K = \begin{pmatrix} -4t & 2\chi_1 ik_2 & 0 & -2\chi_2^* ik_1 \\ -2\chi_1 ik_2 & 4t & 2\chi_2^* ik_1 & 0 \\ 0 & -2\chi_2 ik_1 & -4t & -2\chi_1 ik_2 \\ 2\chi_2 ik_1 & 0 & 2\chi_1 ik_2 & 4t \end{pmatrix} \quad (\text{B4})$$

where  $(k_1, k_2) = \vec{k} - K$ .

In the presence of a vortex  $\chi_2 \rightarrow \chi_2(\vec{x}) = |\chi_2|e^{-i\theta(\vec{x})}$ . Eq. (B4), in real space, becomes

$$H_K = -4t\mu_3 + 2i\chi_1\mu_2\tau_3\partial_2 - 2i|\chi_2|e^{i\frac{\theta}{2}\tau_3}\mu_2\tau_1e^{-i\frac{\theta}{2}\tau_3}\partial_1. \quad (\text{B5})$$

Here the Pauli matrices  $\vec{\mu}$  mix the sublattice labels and  $\vec{\tau}$  mixes particle and hole. One can perform a series of rotations to transform  $H_K$  into a more familiar form (a form that has been studied before<sup>36</sup>):

$$\begin{aligned} \tilde{H}_K &= 4t(\cos\theta\tau_1 + \sin\theta\tau_2) - 2i(|\chi_2|\mu_1\tau_3\partial_1 + \chi_1\mu_2\tau_3\partial_2) \\ &\equiv 4t(\cos\theta\tau_1 + \sin\theta\tau_2) - 2i(\mu_1\tau_3\tilde{\partial}_1 + \mu_2\tau_3\tilde{\partial}_2) \end{aligned} \quad (\text{B6})$$

where we define  $\tilde{\partial}_1 = 2|\chi_2|\partial_1$  and  $\tilde{\partial}_2 = 2\chi_1\partial_1$ .

The transformations that lead from Eq. (B5) to Eq. (B6) are the following. Firstly we perform a rotation along  $\tau_1$  such that  $\tau_3 \rightarrow -\tau_2$ . Afterwards we perform another rotation along  $\mu_1$  such that  $\mu_3 \rightarrow -\mu_2$ ,  $\mu_2 \rightarrow \mu_3$ . After these transformations

$$H_K \rightarrow 4t\mu_2 - 2i\chi_1\tau_2\mu_3\partial_1 - 2i|\chi_2|e^{-i\theta/2\tau_2}\tau_1\mu_3e^{i\theta/2\tau_2}\partial_2 \quad (\text{B7})$$

Second, we perform the rotation  $e^{-i\theta/2\tau_2}e^{i\theta/2\mu_3}$ . Although this rotation is spacial dependent, it commutes with  $\vec{\partial}$  in the long wavelength limit. Another worth noting fact is that  $e^{-i\theta/2\tau_2}e^{i\theta/2\mu_3}$  has no branch cut since for both  $\theta = 0$  and  $\theta = 2\pi$ ,  $e^{-i\theta/2\tau_2}e^{i\theta/2\mu_3} = 1$ . After the above transformation

$$H_K \rightarrow 4t(\cos\theta\mu_2 - \sin\theta\mu_1) - 2i(\chi_1\tau_2\mu_3\partial_1 + |\chi_2|\tau_1\mu_3\partial_2) \quad (\text{B8})$$

After interchanging  $\vec{\mu} \leftrightarrow \vec{\tau}$  and redefining  $\theta \rightarrow \theta + \pi/2$  we obtain Eq. (B6).

In Ref.<sup>36</sup> it is shown that Eq. (B6) has one zero mode. Similarly one can show there is another zero mode associated with  $K^*$ . And same analysis can be applied to anti-vortex. We thus established the two mid-gap modes in the SC vortex (anti-vortex). Their existence ensures the existence of the four low energy spinful vortices discussed in Sec.I.

Next, we analyze a different limit of parameters:  $|\chi_1| \sim 1$ ,  $|t| \sim 1$  and  $|\chi_2| \ll 1$ . Since it is possible to adiabatically tune the parameter from the previous regime to this limit, while preserving  $90^\circ$  rotation and  $PH$  symmetries, we expect the zero modes to survive. In specific, in the previous limit the two zero modes are associated with two different nodes (for small  $t$  and slowly varying  $\theta(\mathbf{x})$  momentum is approximately conserved), and transform into each other under  $90^\circ$  rotation. By forming symmetric and anti-symmetric combination of the two zero modes we obtain two new ones that transform under  $90^\circ$  with s and d symmetries respectively. On the other hand  $PH$  does not change angular momentum, and transforms each mode into its particle-hole conjugate hence reverse the sign of energy. Since the entire adiabatic process preserves the  $90^\circ$  rotation and  $PH$  symmetries, the in-gap states can not shift away from zero energy. We have performed numerical study of the vortices in this parameter limit and find the mid-gap modes.

The reason we are interested in the second limit is because it gives rise to an interesting situation where zero mode arise from a non-Dirac like cone. In the limit of  $|\chi_2| \rightarrow 0$  two *quadratically dispersed bands* touch at a single  $X$  point (see Fig.9). Nonzero  $|\chi_2|$  opens up a gap. To quadratic order in momentum departure from  $X$  the Hamiltonian looks like:

$$H_X = \begin{pmatrix} t(k_2^2 - k_1^2) & -\chi_1 k_1 k_2 & 0 & -4\chi_2^* \\ -\chi_1 k_1 k_2 & -t(k_2^2 - k_1^2) & -4\chi_2^* & 0 \\ 0 & -4\chi_2 & t(k_2^2 - k_1^2) & \chi_1 k_1 k_2 \\ -4\chi_2 & 0 & \chi_1 k_1 k_2 & -t(k_2^2 - k_1^2) \end{pmatrix} \quad (\text{B9})$$

where  $(k_1, k_2) = \vec{k} - X$ . The existence of zero modes when there is a vortex in  $\chi_2$  is very interesting. For up to present all known zero modes are associated with ‘‘mass vortex’’ in Dirac-like equations. The fact that Eq. (B9) is non-relativistic, yet in the presence of ‘‘gap vortices’’ there are zero modes suggest a new type of ‘‘index theorem’’: For one vortex in  $\chi_2$  of Eq.(B9) there are two zero modes.

### APPENDIX C: SYMMETRY ANALYSIS FOR THE SLAVE ROTOR THEORY

In this appendix we study the symmetries of the slave rotor theory. As discussed in appendix V, the relation between the electron operator and the slave rotor and spinon operator is given by<sup>37</sup>:

$$\begin{pmatrix} c_{i\uparrow} & \eta_i c_{i\downarrow}^\dagger \\ c_{i\downarrow} & -\eta_i c_{i\uparrow}^\dagger \end{pmatrix} = \begin{pmatrix} f_{i\uparrow} & \eta_i f_{i\downarrow}^\dagger \\ f_{i\downarrow} & -\eta_i f_{i\uparrow}^\dagger \end{pmatrix} \begin{pmatrix} z_{i1} & z_{i2} \\ -z_{i2}^\dagger & z_{i1}^\dagger \end{pmatrix}, \quad (\text{C1})$$

or equivalently Eq.(28):

$$\begin{aligned} c_{i\uparrow} &= f_{i\uparrow} z_{i1} - \eta_i f_{i\downarrow}^\dagger z_{i2}^\dagger \\ c_{i\downarrow} &= f_{i\downarrow} z_{i1} + \eta_i f_{i\uparrow}^\dagger z_{i2}^\dagger. \end{aligned} \quad (\text{C2})$$

According to the above equation one can insert a site-dependent  $SU(2)$  matrix and its inverse between the  $f$ -spinon and  $z$ -rotor matrices while leave the electron operators invariant. In terms of  $f$ -spinon and  $z$ -boson this local  $SU(2)$  transformation is:

$$\begin{aligned}\psi_i &= \begin{pmatrix} f_{i\uparrow}^\dagger \\ \eta_i f_{i\downarrow} \end{pmatrix} \rightarrow e^{i\alpha_i \cdot \frac{\sigma}{2}} \cdot \psi_i \\ Z_i &= \begin{pmatrix} z_{i1} \\ -z_{i2} \end{pmatrix} \rightarrow e^{i\alpha_i \cdot \frac{\sigma}{2}} \cdot Z_i.\end{aligned}\quad (\text{C3})$$

The above  $SU(2)$  gauge symmetry is broken by the form of the mean-field spin-Hall insulator Hamiltonian of the spinon (Eq. (2)). The remanent gauge symmetry is  $U(1)$ ,

$$f_{i\alpha} \rightarrow e^{i\theta_i} f_{i\alpha} \quad z_{ia} \rightarrow e^{-i\theta_i} z_{ia}.\quad (\text{C4})$$

Due to this remanent  $U(1)$  symmetry, the fluctuation around the mean-field theory appear in the form of a  $U(1)$  gauge theory. We have shown in appendix V that if the  $U(1)$  gauge field is in the Coulomb phase, the spin-Hall insulating properties of the spinon indicates that this is actually the XY ordered phase. This is because the spin-Hall response implies that the photon of the gauge field is actually the Goldstone mode of the XY ordered, as has been shown in text. In the following we study the man-

ifestation of various physical symmetry of the AF phase in the slave-rotor gauge theory.

There are two physical global  $U(1)$  symmetries: the global spin ( $S_z$ ) rotation, and the charge- $U(1)$  symmetry. They are manifested in the slave-rotor theory as:

$$\begin{aligned}S_z \text{ rotation by } \theta: f_{i\uparrow} &\rightarrow e^{i\theta/2} f_{i\uparrow} & f_{i\downarrow} &\rightarrow e^{-i\theta/2} f_{i\downarrow} \\ z_{ia} &\rightarrow z_{ia} \\ \Rightarrow c_{i\uparrow} &\rightarrow e^{i\theta/2} c_{i\uparrow} & c_{i\downarrow} &\rightarrow e^{-i\theta/2} c_{i\downarrow},\end{aligned}\quad (\text{C5})$$

and

$$\begin{aligned}\text{charge-}U(1): f_{i\alpha} &\rightarrow f_{i\alpha} \\ z_{i1} &\rightarrow e^{i\theta} z_{i1} & z_{i2} &\rightarrow e^{-i\theta} z_{i2}. \\ \Rightarrow c_{i\uparrow} &\rightarrow e^{i\theta} c_{i\uparrow} & c_{i\downarrow} &\rightarrow e^{i\theta} c_{i\downarrow}.\end{aligned}\quad (\text{C6})$$

These equation imply  $z_1$  and  $z_2$  are spin zero charge-carrying particles.

Next we study discrete symmetries. Before doing so it is convenient to write the mean-field spinon Hamiltonian in the  $SU(2)$  form. In this form any transformation which changes the mean-field Hamiltonian by a  $SU(2)$  gauge transformation is regarded as a symmetry operation due to the gauge redundancy. Eq.(2) can be rewritten as:

$$H_{TBI} = \sum_{\langle ij \rangle} \psi_i^\dagger \begin{pmatrix} -\chi_{ij}^* & 0 \\ 0 & -\chi_{ij} \end{pmatrix} \psi_j + \sum_{\langle\langle ij \rangle\rangle} \psi_i^\dagger \begin{pmatrix} -t_{ij} & 0 \\ 0 & -t_{ij} \end{pmatrix} \psi_j + h.c. \equiv \psi_i^\dagger U_{ij} \psi_j + h.c. \quad (\text{C7})$$

Under a  $SU(2)$  gauge transformation ,i.e.,  $\psi_i \rightarrow W_i \psi_i$ ,

$$U_{ij} \rightarrow W_i^\dagger U_{ij} W_j. \quad (\text{C8})$$

The  $SU(2)$  gauge invariant quantities are

$$\text{Tr} [U_{\chi_{i,i+\hat{x}}} U_{t_{i+\hat{x},i+\hat{y}}} U_{\chi_{i+\hat{y},i}}] = -2t \cos 2\phi. \quad (\text{C9})$$

for every triangular loop  $i \rightarrow i + \hat{x} \rightarrow i + \hat{y} \rightarrow i$ . Two mean-field Hamiltonians with the same loop trace are related to each other by an  $SU(2)$  gauge transformation.

Now we are ready analyze the discrete symmetries. First, it is obvious that the  $90^\circ$  rotation around the center of each plaquette  $\mathcal{R}_{90}$  is a symmetry since it leaves Eq. (2) invariant. Under this operation the  $z$  bosons transform as:

$$\mathcal{R}_{90}: z_{i1} \rightarrow z_{\mathcal{R}_{90}(i),1} \quad z_{i2} \rightarrow z_{\mathcal{R}_{90}(i),2}. \quad (\text{C10})$$

Next we consider the reflection  $\mathcal{P}$  about the vertical/horizontal lines passing through the center of each plaquette. Naively one would claim that this is not a symmetry of Eq. (2) because

$$\mathcal{P}: \chi \rightarrow \chi^*, t \rightarrow t. \quad (\text{C11})$$

But this is actually a symmetry transformation because it does not change loop trace; one just needs to perform a global  $SU(2)$  gauge transformation  $W_i = i\sigma_2$  (see Eq.(C3)) to restore Eq. (2). Thus reflection,  $\mathcal{P}$ , is a symmetry. Under  $\mathcal{P}$  the  $z$  bosons transform as(see Eq.(C3)):

$$W \circ \mathcal{P}: z_{i1} \rightarrow z_{\mathcal{P}(i),2}^\dagger, \quad z_{i2} \rightarrow -z_{\mathcal{P}(i),1}^\dagger. \quad (\text{C12})$$

This is consistent with the result Eq.(G2). Next, come the particle-hole transformation  $PH$ . According to Ref.<sup>37</sup>, this transformation is implemented on the  $z$ -boson via

$$\begin{aligned}PH: f_{i\alpha} &\rightarrow f_{i\alpha} & z_{i1} &\rightarrow z_{i2} & z_{i2} &\rightarrow -z_{i1}. \\ \Rightarrow c_{i\uparrow} &\rightarrow \eta_i c_{i\downarrow}^\dagger & c_{i\downarrow} &\rightarrow -\eta_i c_{i\uparrow}^\dagger\end{aligned}\quad (\text{C13})$$

Again, this transformation law is consistent with result in Eq.(G1). This transformation also preserves a gapped  $z$  boson action and Eq. (2) hence is a symmetry. Now we consider the translation  $T$ :

$$T_{x/y}: f_i \rightarrow f_{i+x/y}, \quad z_i \rightarrow z_{i+x/y}, \quad c_{i\sigma} \rightarrow c_{i+x/y\sigma}. \quad (\text{C14})$$



Under this operation the parameters in Eq. (2) transform as:

$$T: \chi \rightarrow \chi^*, t \rightarrow -t. \quad (\text{C15})$$

This causes the loop trace to change sign (i.e.,  $-2t \cos 2\phi \rightarrow 2t \cos 2\phi$ ) hence  $T$  is broken by Eq. (2). Next, we proceed to time reversal  $\mathcal{TR}$ . Under time reversal

$$\begin{aligned} \mathcal{TR}(\text{anti-unitary}): f_{i\alpha} &\rightarrow (i\sigma^2)_{\alpha\beta} f_{i\beta}, \quad z_{ia} \rightarrow z_{ia} \\ \Rightarrow c_{i\uparrow} &\rightarrow c_{i\downarrow}, \quad c_{i\downarrow} \rightarrow -c_{i\uparrow} \end{aligned} \quad (\text{C16})$$

Under the above transformation the parameters of Eq. (2) change according to

$$\mathcal{TR}: \chi \rightarrow \chi^*, t \rightarrow -t, \quad (\text{C17})$$

which also flips sign of the loop trace. Hence  $\mathcal{TR}$  is also broken by Eq. (2).

Next we study the compound operation  $T \circ \mathcal{TR}$ . Combining Eq.(C15,C17) it is simple to show that Eq. (2) is invariant under this transformation. Thus we conclude  $T \circ \mathcal{TR}$  is a good symmetry. Using Eq.(C14,C16) we obtain the  $z$  boson transformation law as

$$T \circ \mathcal{TR} : z_{i1} \rightarrow z_{i+1,1}, \quad z_{i2} \rightarrow z_{i+1,2}. \quad (\text{C18})$$

Once again, this is consistent with Eq.(G3).

Because the slave-rotor theory does not capture the  $S_z$  rotation symmetry breaking at the mean-field level, it appears that  $\mathcal{R}_{90}$ ,  $\mathcal{P}$ ,  $PH$ ,  $T \circ \uparrow \leftrightarrow \downarrow$  and  $T \circ \mathcal{TR}$  are always good symmetries. After the breaking of the  $S_z$  rotation the above symmetries might be modified; after the operation of the discrete symmetries it might require an additional  $S_z$  rotation to restore the ground state. For example  $\mathcal{R}_{90}$  and  $\mathcal{P}$  are modified to  $e^{i\pi S_z} \circ \mathcal{R}_{90}$  and  $e^{i\pi S_z} \circ \mathcal{P}$  due to the AF order. For example, the angle of the  $S_z$  rotation can be determined as follows. Assume

$$e^{i\theta S_z} \circ \mathcal{R}_{90} |GS\rangle = |GS\rangle \quad (\text{C19})$$

we obtain

$$\begin{aligned} \langle GS | S_i^\dagger | GS \rangle &= \langle GS | (e^{i\theta S_z} \circ \mathcal{R}_{90}) S_i^\dagger (e^{i\theta S_z} \circ \mathcal{R}_{90})^{-1} | GS \rangle \\ &= e^{-i\theta} \langle GS | S_{\mathcal{R}_{90}(i)}^\dagger | GS \rangle = -e^{-i\theta} \langle GS | S_i^\dagger | GS \rangle, \end{aligned} \quad (\text{C20})$$

hence  $\theta = \pi$ . After some simple calculation it can be shown that in the antiferromagnetic state  $PH$  and  $T \circ \mathcal{TR}$  alone remain good symmetries. Finally, since  $T \circ \uparrow \leftrightarrow \downarrow$  transforms XY order parameter  $M$  to  $-M^*$  (note how the nature of the AF order enters), the associated  $S_z$  rotation must rotate  $-M^*$  back to  $M$ .

In summary, in the AF phase we find while  $T$  and  $\mathcal{TR}$  are broken,  $e^{i\pi S_z} \circ \mathcal{R}_{90}$ ,  $e^{i\pi S_z} \circ \mathcal{P}$ ,  $T \circ \mathcal{TR}$  and  $PH$  are good symmetries. This is consistent with a regular easy-plane

AF ordered state with  $PH$  symmetry. Thus the AF phase portrayed by the slave-rotor+ gauge fluctuation theory is the regular AF phase.

#### APPENDIX D: A MEAN-FIELD THEORY FOR THE AF PHASE AND THE ANALYSIS OF THE CORE STRUCTURE OF THE AF VORTICES

In the main text we have started with a mean-field superconductor and show its vortices carries spin. The condensation of these vortices destroy the superconductor and drive the system into an insulating easy-plane antiferromagnet. The vortices of this antiferromagnet carries charge and their condensation destroys the AF order and drives the system back to the superconducting phase. In section C we have presented a gauged slave rotor theory for this antiferromagnet. In this appendix we present a mean-field Hamiltonian for this phase and study its vortices.

From Sec.C we have shown the symmetries of the AF phase are charge- $U(1)$ ,  $e^{i\pi S_z} \circ \mathcal{R}_{90}$ ,  $e^{i\pi S_z} \circ \mathcal{P}$ ,  $PH$ ,  $T \circ \mathcal{TR}$ . These symmetries severely limit the possible quadratic mean-field Hamiltonians. The most general quadratic Hamiltonian can be written as combination of hopping terms (however in general the hopping does not have to conserve the spin). Demanding the above symmetries it is possible to write down all symmetry allowed hopping terms. For example consider the nearest neighbor hopping. We shall show in the following that the only symmetry allowed such hopping term is of the form  $\chi_1 (c_{i\sigma}^\dagger c_{j\sigma} + h.c.)$  where  $\chi_1$  is a real number. Let us first assume the up spin hopping amplitude is imaginary:  $i\lambda c_{i\uparrow}^\dagger c_{j\uparrow} + h.c.$ . Under  $PH$  transformation it becomes  $-i\lambda c_{i\downarrow}^\dagger c_{j\downarrow} + h.c. = i\lambda c_{j\downarrow}^\dagger c_{i\downarrow} + h.c. = -i\lambda c_{i\downarrow}^\dagger c_{j\downarrow} + h.c.$  Hence the spin up and spin down hopping matrix elements must differ by a sign, i.e.,  $i\sigma (c_{i\sigma}^\dagger c_{j\sigma} - c_{j\sigma}^\dagger c_{i\sigma}) + h.c.$ . Because the sign difference between  $i \rightarrow j$  and  $j \rightarrow i$ , this hopping has a direction. Let us represent the direction in which the hopping amplitude is  $i\lambda$  by an arrow.  $T \circ \mathcal{TR}$  requires the arrows to be translation invariant, but this breaks the  $e^{i\pi S_z} \circ \mathcal{R}_{90}$ . So the imaginary spin preserving nearest neighbor hopping is forbidden. Next let us consider the spin flipping nearest neighbor hopping  $M^* c_{i\uparrow}^\dagger c_{j\downarrow} + h.c.$ .  $PH$  transforms it into  $M^* c_{i\downarrow}^\dagger c_{j\uparrow} + h.c. = -M^* c_{j\uparrow}^\dagger c_{i\downarrow} + h.c.$  Thus the hopping also has a direction, i.e., the hopping amplitude for  $c_{i\uparrow}^\dagger c_{j\downarrow}$  is the negative of that of  $c_{j\uparrow}^\dagger c_{i\downarrow}$ . The  $T \circ \mathcal{TR}$  requires the hopping to be translation invariant, but this again must break the  $e^{i\pi S_z} \circ \mathcal{R}_{90}$ . So the spin flipping nearest neighbor hopping is also forbidden. This leaves the regular real-amplitude spin-preserving hopping as the only possibility.

One can perform similar analysis for all possible quadratic terms: on-site terms, nearest neighbor terms, next nearest neighbor terms, etc. The following Hamiltonian has the most general form up to second neighbor:

$$H_{AF}^{MF} = \sum_i \eta_i (M_1^* c_{i\uparrow}^\dagger c_{i\downarrow} + h.c.) + \chi_1 \sum_{\langle ij \rangle} (c_{i\sigma}^\dagger c_{j\sigma} + h.c.) + \sum_{\langle\langle ik \rangle\rangle} t_{ik} (\sigma c_{i\sigma}^\dagger c_{k\sigma} + h.c.) + \sum_{\langle\langle ik \rangle\rangle} \eta_i M_2^* (c_{i\uparrow}^\dagger c_{k\downarrow} + c_{k\uparrow}^\dagger c_{i\downarrow}) + h.c. \quad (D1)$$

where  $t_{ij}$  has the staggered pattern as shown in Fig.1(a).

Interestingly it is not possible to choose parameters so that Eq.(D1) will have conic (i.e., Dirac-like) intersecting bands. If one set  $M_1 = M_2 = 0$ , the two bands intersect

quadratically at  $X$  point. Small  $M_1$  and/or  $M_2$  open up a gap. In this limit the momentum space Hamiltonian around  $X$  is

$$H_{AF,X}^{MF} = \Psi_k^\dagger \begin{pmatrix} t(k_2^2 - k_1^2) & -\chi_1 k_1 k_2 & M^* & 0 \\ -\chi_1 k_1 k_2 & -t(k_2^2 - k_1^2) & 0 & -M^* \\ M & 0 & -t(k_2^2 - k_1^2) & -\chi_1 k_1 k_2 \\ 0 & -M & -\chi_1 k_1 k_2 & t(k_2^2 - k_1^2) \end{pmatrix} \Psi_k \quad (D2)$$

where  $(k_1, k_2) = \vec{k} - X$ ,  $M = M_1 - 2M_2$  and

$$\Psi_k^\dagger = (c_{A\uparrow k}^\dagger, c_{B\uparrow k}^\dagger, c_{A\downarrow k}^\dagger, c_{B\downarrow k}^\dagger). \quad (D3)$$

After a simple unitary rotation:

$$\Psi_k \rightarrow \begin{pmatrix} \mathbf{1} & 0 \\ 0 & i\sigma_2 \end{pmatrix} \Psi_k \quad (D4)$$

The form of the Hamiltonian becomes the same form as Eq.(B9) in appendix B. Based on the index theorem obtained there, we conclude one vortex (antivortex) in  $M$  also has two mid-gap energy levels. If both levels are filled the vortex (anti-vortex) carries electric charge 1, and if both are empty the vortex (anti-vortex) carries charge  $-1$ . This is because the vortex with both levels filled and the vortex with both levels empty are related by  $PH$  and thus their charges differ by sign change. On the other hand by definition these two vortices' charges differ by 2. We thus prove the existence of the charge- $\pm 1$  vortex (anti-vortex) in the AF phase.

#### APPENDIX E: THE MATRIX ELEMENT OF THE ORDER PARAMETER OPERATOR (VORTEX TUNNELING OPERATOR) IN SC AND AF PHASES

The SC $\leftrightarrow$ AF transition is realized by condensing vortices with non-trivial quantum number. The motivation of studying the vortex tunneling operator is to compute the order pattern in the vortex condensed phase. The calculation presented here provides a rigorous and systematical way to determine the order pattern in the vortex condensed phase. As a first application, let us study the vortices in the SC phase to show that the vortex condensed phase is AF.

What is the order parameter in the SC vortex  $|\langle \Psi_\uparrow \rangle| = |\langle \Psi_\downarrow \rangle| \neq 0$  condensed phase? Apparently both  $\langle \Psi_\uparrow \rangle$  and  $\langle \Psi_\downarrow \rangle$  are non-zero and one may think that there are two spin-1/2 order parameters. However both  $\Psi_\uparrow$  and  $\Psi_\downarrow$  are non-local operators (since they annihilate vortices of the SC phase) hence can not serve as order parameter. However the combination  $\Psi_\uparrow^\dagger \Psi_\downarrow$  (which does not change vorticity but flips spin) is local, and acquires non zero value in the XY ordered state, hence can serve as an order parameter. To determine the nature (i.e. FM versus AF) of the XY order, we compute the quantum number of the  $\Psi_\uparrow^\dagger \Psi_\downarrow$  operator. For example, if  $\Psi_\uparrow^\dagger \Psi_\downarrow$  changes sign under a 90 degree rotation ( $\mathcal{R}_{90}$ ) around the center of a plaquette, it is consistent with AF order.

In order to determine the quantum number of the operator  $\Psi_\uparrow^\dagger \Psi_\downarrow$  we consider the two vortex states  $|AV_\uparrow\rangle$  and  $|BV_\downarrow\rangle$  with the location of the vortices displaced from one another by one lattice spacing. However we tune the parameters so that the core size  $\xi$  of the vortices is significantly larger than their separation. As shown in Sec.B, there are two spin-up in-gap levels in the vortex core, and  $AV_\uparrow$  and  $BV_\downarrow$  differ by whether the two levels are filled or not. If  $\gamma_{1\uparrow}^\dagger$  and  $\gamma_{2\uparrow}^\dagger$  create Bogoliubov quasiparticle in these levels, then in the limit  $\xi \gg 1$   $|AV_\uparrow\rangle = \gamma_{1\uparrow}^\dagger \gamma_{2\uparrow}^\dagger |BV_\downarrow\rangle$ . On the other hand from Eq. (A1) we know that the operator  $\Psi_\uparrow^\dagger \Psi_\downarrow$  sends  $BV_\downarrow$  to  $AV_\uparrow$ , i.e., *it is the vortex tunneling operator*:

$$|AV_\uparrow\rangle = \Psi_\uparrow^\dagger \Psi_\downarrow |BV_\downarrow\rangle. \quad (E1)$$

Therefore the quantum number of  $\Psi_\uparrow^\dagger \Psi_\downarrow$  is simply the quantum number difference of  $|AV_\uparrow\rangle$  and  $|BV_\downarrow\rangle$ . For example let us consider the rotation  $\mathcal{R}_{90}$ . If the vortex configuration is symmetric under  $\mathcal{R}_{90}$  we expect  $|AV_\uparrow\rangle$

and  $|BV_\downarrow\rangle$  to be eigenstates of  $\mathcal{R}_{90}$ :

$$\begin{aligned}\mathcal{R}_{90}|AV_\uparrow\rangle &= e^{i\theta_\uparrow}|AV_\uparrow\rangle \\ \mathcal{R}_{90}|BV_\downarrow\rangle &= e^{i\theta_\downarrow}|BV_\downarrow\rangle\end{aligned}\quad (\text{E2})$$

To determine the quantum number difference,  $e^{i(\theta_\uparrow-\theta_\downarrow)}$ , we can calculate the following matrix element ratio

$$\frac{\langle AV_\uparrow|S_i^+|BV_\downarrow\rangle}{\langle AV_\uparrow|S_j^+|BV_\downarrow\rangle}.\quad (\text{E3})$$

To see that let us consider  $j = \mathcal{R}_{90}(i)$  and thus  $S_j^+ = \mathcal{R}_{90}^{-1}S_i^+\mathcal{R}_{90}$ . In this case Eq.(E3) becomes

$$\frac{\langle AV_\uparrow|S_i^+|BV_\downarrow\rangle}{\langle AV_\uparrow|\mathcal{R}_{90}^{-1}S_i^+\mathcal{R}_{90}|BV_\downarrow\rangle} = e^{i(\theta_\uparrow-\theta_\downarrow)}.\quad (\text{E4})$$

From the above it is clear that one can replace the  $S_i^\dagger$  in Eq. (E4) by any spin-1 operator  $\hat{O}_i$  and get the same result so long as  $\langle AV_\uparrow|\hat{O}_i|BV_\downarrow\rangle \neq 0$ .

In Eq.(E4) we have assumed that the vortex configuration is  $\mathcal{R}_{90}$ -symmetric so that  $|AV_\uparrow\rangle$  and  $|BV_\downarrow\rangle$  are eigenstates of  $\mathcal{R}_{90}$ . The easiest way to implement the 90-degree rotation symmetry is to put in a vortex under open boundary condition. However this brings in edge states in the gap since the superconductor in question is a topological one. To avoid the complication of edge states it is better to use periodic boundary condition. However in that case one has to put in a vortex and an antivortex hence necessarily breaks the 90 degree rotation symmetry. Fortunately, it turns out that the ratio in Eq. (E3) is almost completely determined by the wavefunctions of the mid-gap levels. The latter is localized in the core region and can only sense a region  $D$  around the center of the vortex. Thus if we separate the vortex and the antivortex by sufficient distance and make sure that the vortex configuration within region  $D$  is rotation symmetric, we expect the matrix element ratio would converge to the desired result  $e^{i(\theta_\uparrow-\theta_\downarrow)}$  in the following limit: (1) large vortex core size (2) large system size ( $D$  size). In practice we input the vortices by Jacobi theta function as discussed in detail in Sec.E and the vortex configuration around the vortex center tends to rotational symmetric in the afore mentioned limit.

In Fig.10 we present the result for  $\langle AV_\uparrow|S_i^+|BV_\downarrow\rangle$  as a function of  $i$  for a fixed vortex configuration. We find in the vortex core the matrix elements have staggered signs, which means the XY order is AF.

We showed  $\Psi_\uparrow^\dagger\Psi_\downarrow$  is an AF order parameter. Here we present some details of the numerics that we performed. In Fig.11 we show the positions of the vortex and the anti-vortex centers on the torus. We use complex number  $w_1, w_2$  to represent the position of the vortex and anti-vortex. Given these positions, and using complex number  $z = x + iy$  to represent the position of the pairing bond center, the pairing amplitude is given by:

$$\Delta(z) = |\Delta_0|e^{i\phi(z)}(1 - e^{-|z-w_1|/\xi})(1 - e^{-|z-w_2|/\xi}),\quad (\text{E5})$$

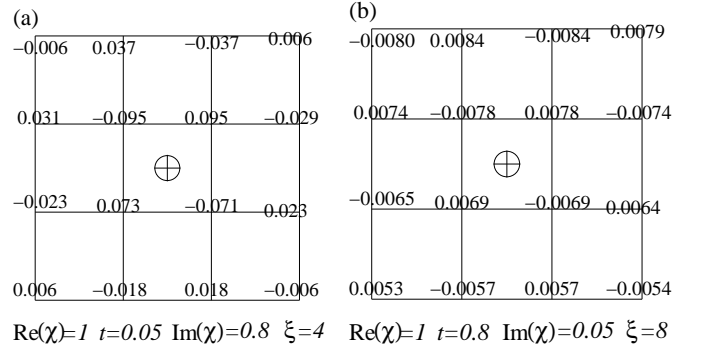


FIG. 10:  $\langle AV_\uparrow|S_i^+|BV_\downarrow\rangle$  as a function of  $i$  for sites close to the center of the vortex (labeled by  $\oplus$ ). We input a vortex and an anti-vortex separated by half system size on a  $24\times 24\times 2$  ('2' means 2 sites per unit cell) system on torus (details of the vortex configurations are given in Sec.E).  $Re(\chi)$ ,  $t$  and  $Im(\chi)$  are the parameters in Eq.(1). To make the core size  $\xi$  big, we input the pairing order parameter in the vicinity of the vortex core as  $Im(\chi)(1 - e^{-r/\xi})e^{i\theta}$ , where  $r, \theta$  are the polar coordinates with respect to the center of the vortex. We used two sets of parameters: (a) large pairing and small  $t$  and (b) small pairing and large  $t$ . In limit (a) the vortex core is relatively small, while (b) the vortex core is large (for details see Sec.B and E). In both limit we see staggered signs, implying AF order.

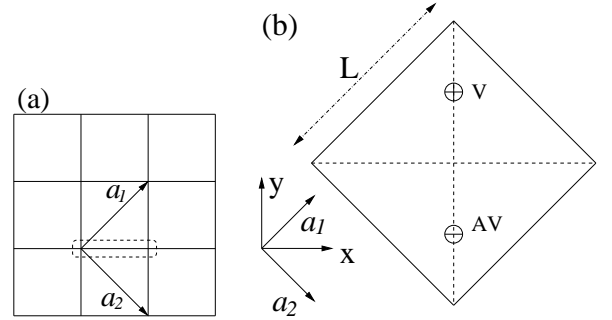


FIG. 11: (a) The real space unit cell of the square lattice model Eq.(1) and the basis vectors  $a_1, a_2$ . (b) In our numerical study, we put one vortex  $\oplus$  and one anti-vortex  $\ominus$  separated by half system size on a sample with periodic boundary conditions.

where  $\xi \ll L$  is the size of the vortex core, and the phase  $\phi(z)$  is given by:

$$\begin{aligned}\phi(z) &= \arg\left(\theta_1\left(\frac{\pi(z-w_1)}{\sqrt{2}L}, e^{i\pi\frac{1+i}{2}}\right)\bar{\theta}_1\left(\frac{\pi(z-w_2)}{\sqrt{2}L}, e^{i\pi\frac{1+i}{2}}\right)\right) \\ &\quad - \frac{2\pi Im(z)}{L^2}Re(w_1 - w_2).\end{aligned}\quad (\text{E6})$$

And the Jacobi theta function is defined as:

$$\theta_1(z, q) = \sum_{n=-\infty}^{\infty} (-1)^{n-\frac{1}{2}} q^{(n+\frac{1}{2})^2} e^{(2n+1)iz}.\quad (\text{E7})$$

One can show that  $e^{i\phi(z)}$  is a periodic function on the  $L\times L$  sample with a vortex and an anti-vortex at  $w_1, w_2$ .

We mention that  $\xi$  determines the input vortex size, but it does not determine the size of the zero mode wavefunction (which actually weakly dependent on  $\xi$ ). We find that size of the zero mode wavefunction is mainly determined by the pairing  $|\Delta_0|$  by numerical study. This behavior at least can be understood in the Dirac limit where the analytical solution of the zero mode wavefunction is known<sup>36</sup> to be  $\sim e^{-|\Delta_0|r}$ . To provide a quantitative understanding of the size of the zero mode wavefunction  $\psi(\vec{r})$  we numerically fit the density  $|\psi(\vec{r})|^2$  by  $Ae^{-\frac{(\vec{r}-\vec{r}_0)^2}{l^2}}$ . We find for the vortex configuration in Fig.10(a) the zero mode size  $l = 1.5$ , and for Fig.10(b)  $l = 6.0$ . This finishes the discussion of the SC vortex tunneling amplitude.

From now on we study the AF vortex tunneling amplitude. We adopt the mean-field Hamilton Eq.(D1) from Sec.D and only consider the on-site magnetization:

$$H_{AF}^{MF} = \sum_i \eta_i (M^* c_{i\uparrow}^\dagger c_{i\downarrow} + h.c.) + \chi \sum_{\langle ij \rangle} (c_{i\sigma}^\dagger c_{j\sigma} + h.c.) + \sum_{\langle ik \rangle} t_{ik} (\sigma c_{i\sigma}^\dagger c_{k\sigma} + h.c.) \quad (\text{E8})$$

From Sec.D we know that there are two zero modes in the vortex core  $\eta_1, \eta_2$  in the long wavelength limit. Therefore there are two charged vortex states  $|V_{Q=1}\rangle$  and  $|V_{Q=-1}\rangle$  are related by  $|V_{Q=1}\rangle = \eta_1^\dagger \eta_2^\dagger |V_{Q=-1}\rangle$ . On the other hand because the  $z$ -bosons in Eq.(13) is the relativistic boson fields of these vortices and anti-vortices, we conclude that:

$$|V_{Q=1}\rangle = z_1^\dagger z_2 |V_{Q=-1}\rangle \quad (\text{E9})$$

This is because  $z_1^\dagger z_2$  does not change vorticity but create a pair of electrons.  $z_1^\dagger z_2$  is nothing but a cooper pair creation operator. In the  $\langle z_1 \rangle \neq 0, \langle z_2 \rangle \neq 0$  phase  $z_1^\dagger z_2$  acquires non-zero expectation value and it is the SC order parameter. What is the SC order pattern?

To answer this question we perform the following matrix element ratio computation.

$$\frac{\langle V_{Q=1} | (c_{i\uparrow}^\dagger c_{i+\{x,y\}\downarrow}^\dagger - c_{i\downarrow}^\dagger c_{i+\{x,y\}\uparrow}^\dagger) | V_{Q=-1} \rangle}{\langle V_{Q=1} | (c_{i\uparrow}^\dagger c_{j+\{x,y\}\downarrow}^\dagger - c_{j\downarrow}^\dagger c_{i+\{x,y\}\uparrow}^\dagger) | V_{Q=-1} \rangle} \quad (\text{E10})$$

---


$$L_{\text{latt}} = \sum_{i,\sigma} f_i^\dagger (\partial_t + ib_{0,i} - \hbar A_{0,i}^s \sigma^3) f_i + \left[ \sum_{\langle i,j \rangle} e^{i(b_{ij} - A_{ij}^s \sigma^3)} \chi_{ij} f_{i\sigma}^\dagger f_{j\sigma} + \sum_{\langle\langle i,j \rangle\rangle, \sigma} \sigma t_{ij} e^{i(b_{ij} - A_{ij}^s \sigma^3)} f_{i\sigma}^\dagger f_{j\sigma} + h.c. \right]. \quad (\text{F1})$$


---

Physically Eq. (F1) describes a half-filled (i.e., one particle per site) system of fermions, or more precisely, a spin state.

We now show that this theory describes an XY ordered

phase. As discussed in the paragraph containing Eq. (16) the monopole operator serves as the order parameter of

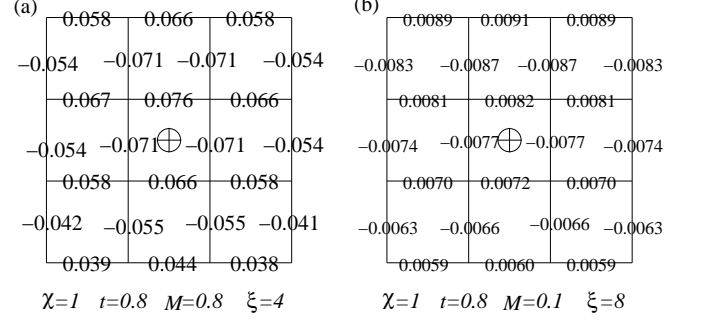


FIG. 12: The AF vortex matrix elements  $\langle V_{Q=1} | (c_{i\uparrow}^\dagger c_{i+\{x,y\}\downarrow}^\dagger - c_{i\downarrow}^\dagger c_{i+\{x,y\}\uparrow}^\dagger) | V_{Q=-1} \rangle$ . We input the vortex and anti-vortex in the same fashion as we did for SC vortex, and choose two sets of parameters: (a) large magnetization with small vortex size, and (b) small magnetization with large vortex size. The staggered sign indicates that the pairing is d-wave in the AF vortex condensed phase.

## APPENDIX F: THE QUANTUM NUMBER OF THE MONOPOLE OPERATOR AND THE MAGNETIC ORDER PATTERN IN THE SLAVE-ROTOR THEORY

In this section we determine the magnetic order pattern in the slave rotor theory. We first show the quantum number of the gauge monopole determines the magnetic order pattern, then we find a way to compute this quantum number. We find the magnetic order pattern is anti-ferromagnetic consistent with the conclusion in the main text.

In the magnetic ordered state, the  $z_\alpha$ 's are absent at long distance/time. Dropping them from the slave-rotor gauge theory we arrive at a spinon theory interacting with a  $U(1)$  gauge field:

phase. As discussed in the paragraph containing Eq. (16) the monopole operator serves as the order parameter of

the magnetic order, i.e., we expect

$$V_D^\dagger \sim \sum_{i \in D} e^{i\theta_i} S_i^+, \quad (\text{F2})$$

where  $D$  is the spatial extent of the monopole (i.e., the region spanned by the inserted gauge flux). We expect  $V_D^\dagger$  to be the antiferromagnetic order parameter hence

$$e^{i\theta_i} = \eta_i \quad (\text{F3})$$

where  $\eta_i$  is the staggered sign. In general there is an arbitrary global phase factor relating  $V_D^\dagger$  to  $\sum_{i \in D} \eta_i S_i^+$ , however this phase does not affect our determination of the the magnetic order.

It is convenient to choose  $D$  and the inserted flux distribution so that they do not break lattice symmetry of Eq. (F1). The transformation properties of  $V_D^\dagger$  under the symmetry operation is what we referred to as the monopole quantum number. As discussed in appendix C the symmetry of Eq. (F1) include rotation  $\mathcal{R}_{90}$  and/or  $T \circ \mathcal{TR}$ . If  $e^{i\theta_i} = 1 \forall i$  (ferromagnetic)  $V_D^\dagger$  would be invariant under  $\mathcal{R}_{90}$ . On the other hand if  $e^{i\theta_i} = \eta_i$  (antiferromagnetic)  $V_D^\dagger$  would change sign under rotation. Thus the transformation property (or the quantum number) of  $V_D^\dagger$  crucially depends on the phase  $e^{i\theta_i}$  (or more precisely on the relative phase  $e^{i(\theta_i - \theta_j)}$  for  $i \in A$  or B sublattices.

How to compute the relative phases? In the following we will show that

$$e^{i(\theta_j - \theta_i)} = \left( \frac{\langle GS, 1\text{-flux} | P S_i^+ P | GS, 0\text{-flux} \rangle}{\langle GS, 1\text{-flux} | P S_j^+ P | GS, 0\text{-flux} \rangle} \right), \quad (\text{F4})$$

where  $|GS, 0\text{-flux}\rangle$  is the spinon mean-field wavefunction of Eq. (2) in zero gauge flux and  $|GS, 1\text{-flux}\rangle$  is the mean-field wavefunction in the background of a uniform flux integrated to one flux quantum.  $P$  is the operator that executes the projection onto the Hilbert space of one-fermion-per-site. This formula of computing the monopole quantum numbers is firstly proposed by one of the authors in Ref.<sup>38</sup> to address the similar issue of the monopole quantum number in a U(1) Dirac spin liquid on a Kagome lattice. One way to understand this formula, is to consider the wavefunction of a monopole condensed phase. Clearly, it is a superposition of different fluxes  $|M\rangle \cong P|0\text{-flux}\rangle + \alpha P|1\text{-flux}\rangle + \alpha^* P|-1\text{-flux}\rangle$ . Hence the expectation value of the spin operator is given by  $\langle M | S_r^+ | M \rangle \sim \langle 0\text{-flux} | P S_r^+ P | 1\text{-flux} \rangle$ .

We have performed numerical calculation of the relative phases in Eq. (F4). Specifically, we fix  $i$ -site to be an arbitrary site on the square lattice and compute  $\theta_j - \theta_i$  as  $j$  varies through the sites of a finite lattice. (We employ the periodic boundary condition in this calculation.) The result for different lattice sizes are illustrated in Fig.(13). We find  $e^{i(\theta_j - \theta_i)}$  is 1 if  $i$  and  $j$  are on the same sublattice and  $-1$  if  $i$  and  $j$  are on different sublattices. Moreover the result is independent of the value of  $\chi$  and  $t$ . This proves that the magnetic order described by Eq. (F1) is *anti-ferromagnetic*.

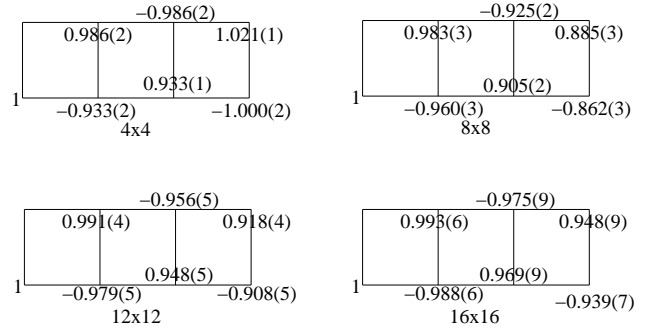


FIG. 13: The numerical result for Eq. (F4) for  $4 \times 4$ ,  $8 \times 8$ ,  $12 \times 12$  and  $16 \times 16$  lattices under periodic boundary condition. We fix  $i$  to be the bottom left site and show the result as  $j$  goes through six different sites as shown. In the limit of large system size the magnitude of the ratio approaches one and the phase factor is 1 for  $i, j$  on the same sublattice and  $-1$  for the opposite sublattices. In constructing this figure we choose parameters  $\Phi = 0.6\pi$ ,  $|t/\chi| = 0.2$  in Eq. (2). The relative phase factors are found to be independent of the parameter values.

In the following we present a discussion of why Eq.(F4) is the right quantity to calculate. As discussed in appendix C symmetry operation is manifested in gauge theory modulo gauge transformation. In other words, any change of the  $f$ -Hamiltonian in Eq. (F1) induced by a transformation that can be undone by a gauge transformation will preserve the gauge theory defined in Eq. (F1). The collection of such compounded transformation form the so-call projective symmetry group (PSG)<sup>39</sup>. However, unlike the physical symmetry operations, the elements of the PSG depends on which gauge the mean-field  $f$ -Hamiltonian is written. Certain gauge are particularly convenient (in the sense that the accompanied gauge transformation is trivial) for some physical symmetry operations (but not for others). However, so long as two gauges are related by a gauge transformation

$$f_{i\sigma} \rightarrow e^{i\phi_i} f_{i\sigma}, \quad \text{where} \quad \prod_i e^{i\phi_i} = 1 \quad (\text{F5})$$

the corresponding PSG operation will yield the same result when acting upon a spin state (i.e., a spinon state with one particle per site). This degrees of freedom works in our favor when we try to determine the symmetry properties of spin state. For example, it allows us to choose the “best gauge” for each different symmetry operation. Thus in order to determine the symmetry property of a spin state (written in spinon variables) one can adapt the “best gauge” for each symmetry operations.

Now we are ready to define the monopole quantum number. Let  $|\Psi, 0\text{-flux}\rangle$  and  $|\Psi, 1\text{-flux}\rangle$  be the ground spin state (written in terms of the spinon variables) with zero and one quantum of background flux, respectively. (By definition  $|\Psi, 1\text{-flux}\rangle = V^\dagger |\Psi, 0\text{-flux}\rangle$ .) The quantum number of  $V^\dagger$  is determined by the relative transformation properties of  $|\Psi, 1\text{-flux}\rangle$  and  $|\Psi, 0\text{-flux}\rangle$  under the elements of PSG (hopefully under the best gauge). Let

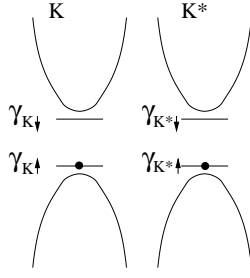


FIG. 14: The in-gap Landau levels when a single quantum of magnetic flux is added to Eq. (2).  $K$  and  $K^*$  mark the momentum space location of the Dirac points when the second neighbor hopping is switched off. For up-spinons the Landau level are close to the top of the valence band, and for down spinons they are close to the bottom of the conduction band. In the depicted filling of Landau levels, the total  $S_z = 1$ .

us again use rotation  $\mathcal{R}_{90}$  as an example. If  $|\Psi, 0\text{-flux}\rangle$  is invariant but  $|\Psi, 1\text{-flux}\rangle$  acquires a phase factor  $e^{i\phi}$  under the appropriate PSG operation

$$\begin{aligned}\mathcal{R}_{90}|\Psi, 0\text{-flux}\rangle &= |\Psi, 0\text{-flux}\rangle \\ \mathcal{R}_{90}|\Psi, 1\text{-flux}\rangle &= e^{i\phi}|\Psi, 1\text{-flux}\rangle,\end{aligned}\quad (\text{F6})$$

then by definition  $V^\dagger$  has a rotational quantum number  $e^{i\phi}$ . Because  $P|GS, 0\text{-flux}\rangle$  and  $P|GS, 1\text{-flux}\rangle$  also describes state with one spinon per site, they also enjoy the best gauge freedom discussed earlier. It is also important to point out that although  $P|GS, 0\text{-flux}\rangle$  and  $P|GS, 1\text{-flux}\rangle$  are not the exact states  $|\Psi, 0\text{-flux}\rangle$  and  $|\Psi, 1\text{-flux}\rangle$ . So long as they have the same PSG transformation property as them, Eq.(F4) (in the thermodynamic limit) will yield the exact monopole quantum number. Again using  $\mathcal{R}_{90}$  as an example we should have

$$\begin{aligned}& \frac{\langle GS, 1\text{-flux} | P S_i^+ P | GS, 0\text{-flux} \rangle}{\langle GS, 1\text{-flux} | P S_{\mathcal{R}_{90}(i)}^+ P | GS, 0\text{-flux} \rangle} \\ &= \frac{\langle GS, 1\text{-flux} | P S_i^+ P | GS, 0\text{-flux} \rangle}{\langle GS, 1\text{-flux} | P \mathcal{R}_{90}^{-1} S_i^+ \mathcal{R}_{90} P | GS, 0\text{-flux} \rangle}.\end{aligned}\quad (\text{F7})$$

The advantage of  $P|GS, 0\text{-flux}\rangle$  and  $P|GS, 1\text{-flux}\rangle$  are that their PSG transformation properties can be read off from those of  $|GS, 0\text{-flux}\rangle$  and  $|GS, 1\text{-flux}\rangle$ .

Even so determine the transformation properties of  $|GS, 0\text{-flux}\rangle$  and  $|GS, 1\text{-flux}\rangle$  can be quite involved. For example if we want to obtain the transformation property of  $|GS, 0\text{-flux}\rangle$  under  $\mathcal{R}_{90}$ , one can choose a gauge (the best gauge) in which the spinon hopping matrix elements are fully translation invariant. In this gauge we expect  $|GS, 0\text{-flux}\rangle$  to be rotation symmetric. However to figure out the symmetry properties of  $|GS, 1\text{-flux}\rangle$ , we face a more challenging situation. For example it is impossible to choose a gauge which preserves the rotation symmetry on torus (because the fluxes through the torus holes are gauge invariant and breaks rotation). Under open boundary condition one can choose the symmetric gauge  $\vec{A} = \frac{1}{2}B\hat{z} \times \vec{r}$  which is rotation invariant. Under

this (best) gauge it is possible to analytically study the transformation law of  $|GS, 1\text{-flux}\rangle$  under rotation. More specifically, due to the topological nature of the spinon mean-field Hamiltonian, one can show that in the presence of one quantum of uniform flux, there are two in-gap Landau levels near the top of the valence band for the up spinons and another two near the bottom of the conduction band for the down spinons. This is illustrated in Fig.14. Because these in-gap levels have definite angular momentum in the symmetric gauge an analytical study of the rotation quantum number is possible. In numerical study of Eq.(F4) one does not need to worry about any of the above; one simply computed in the ratio in the any gauge. We have done just that for the results presented in Fig.13.

## APPENDIX G: SOME SMALL SECTIONS

### 1. Microscopic symmetries and action Eq.(13)

As a double check we show in the following that the validity of action Eq.(13) is ensured by microscopic symmetries. We should check that under symmetry transformations (1)  $z_1 \rightarrow z_2$  (2)  $z \rightarrow z^\dagger$  (which ensures theory to be relativistic.), and (3)  $z_1$  and  $z_2$  particles do not experience any background magnetic field. In the AF phase the spin  $S_z$  rotation is broken and charge- $U(1)$ ,  $PH$ ,  $T \circ \mathcal{TR}$  remains good symmetries. Due to the antiferromagnetic order, reflection  $\mathcal{P}$  has to be followed by a  $\pi$  spin  $S_z$  rotation, i.e.,  $\mathcal{P} \rightarrow e^{i\pi S_z} \circ \mathcal{P}$  so that the ground state will be preserved.

$PH$  transforms a spin vortex into a vortex and flip the charge, therefore

$$PH: z_1 \rightarrow z_2, z_2 \rightarrow z_1 \quad (\text{G1})$$

Under  $e^{i\pi S_z} \circ \mathcal{P}$  a vortex is transformed into an anti-vortex while preserving the charge, thus we have

$$e^{i\pi S_z} \circ \mathcal{P}: z_1 \rightarrow z_2^\dagger, z_2 \rightarrow z_1^\dagger \quad (\text{G2})$$

Eq.(G1,G2) ensures condition (1) and (2).  $T \circ \mathcal{TR}$  transforms a vortex into a vortex while preserving the charge:

$$T \circ \mathcal{TR}: z_1 \rightarrow z_1 \quad z_2 \rightarrow z_2 \quad (\text{G3})$$

Although  $z_\alpha$  transform trivially under  $T \circ \mathcal{TR}$ , it is important to bare in mind that because it is an anti-unitary transformation it changes sign of  $a_\mu$  in Eq. (13). This ensures condition (3).

### 2. The edge modes of the topological superconductor

Since the rotation Eq.(3) preserves the spectrum of the Hamiltonian, we can use the existence of gapless edge states in TBI to imply the same for the SC. Moreover

since the rotation preserves the spin, we conclude that, as in TBI, the edge modes in the superconductor must have opposite spin propagate in opposite direction. However unlike the edge mode in TBI, that of the superconductor do not carry definite charge.

It is important to ask under what condition are these edge modes stable. In the TBI phase it is the charge and spin conservation law that guarantee the stability. Translated into the SC, spin conservation law remains the same but the charge conservation law becomes the conservation of  $\sum_i \eta_i (c_{i\uparrow} c_{i\downarrow} + h.c.)$ , does not seem to be a physical conservation law for a realistic system. Fortunately it turns out that the particle-hole symmetry plus the  $S_z$  conservation are sufficient to guarantee the stability of the gapless edge modes in the SC phase.

This is easily seen as follows. Particle hole symmetry is implemented by  $\psi_r \rightarrow i\mu_x \psi_r$ . For convenience, let us translate this into the spinon variables where it implies  $F_r \rightarrow Z_r i\mu_x Z_r^\dagger F_r$ , which is  $F_r \rightarrow i\mu_z F_r$  in a particular gauge. If the quadratic Hamiltonian of the  $F_r$  is invariant under this transformation, then it should only depend on the identity and  $\mu_z$ . This implies it has a  $U(1)$  rotation symmetry corresponding to spinon number conservation. Combined with  $U(1)$  spin rotation invariance, this is sufficient to protect the edge modes.

### 3. Physical Interpretation of the doublet of Chargeons

Since the preceding justification for introducing a charged boson doublet is rather formal, phrased in terms of gauge theories and symmetries, we provide here a more physical motivation for the appearance of the pair of fields  $z_1, z_2$ . Consider an insulating state composed of local moments described by a fermionic mean field theory as in 25. Consider introducing charge fluctuations by including electron excitations  $c_r^\dagger$ . In a single band model, these electrons or holes will form a singlet with the spin on that site. Hence, if we consider low energy charge excitations which are spin singlets, then one can construct two different operators  $b_1 = c_\sigma^\dagger f_\sigma$  and  $b_2^\dagger = \epsilon_{\sigma\sigma'} c_{\sigma'}^\dagger f_\sigma^\dagger$ , where  $\epsilon_{\sigma\sigma'}$  is the antisymmetric symbol and a sum on spin indices is assumed. Keeping in mind the constraint 22 one can readily show that these bosonic operators satisfy:

$$\begin{aligned} c_\uparrow &= b_1 f_\uparrow - f_\downarrow^\dagger b_2^\dagger \\ c_{r\downarrow} &= b_1 f_{r\downarrow} + f_\uparrow^\dagger b_2^\dagger \end{aligned} \quad (G4)$$

clearly these are very similar to the  $z_1, z_2$  fields. Moreover, one can check that the on site Cooper pair operator:  $\epsilon_{\sigma\sigma'} c_\sigma^\dagger c_{\sigma'}^\dagger = b_1 b_2^\dagger$ . Hence, one can consider these operators as a 'Schwinger boson' representation of the Cooper pair.

## APPENDIX H: XY $\leftrightarrow$ SC DIRECT TRANSITION ON THE HONEYCOMB LATTICE

From the vortex core zero mode study (see Sec.I~IV) we found there is a direct transition from AF phase to d-wave SC phase on square lattice. However that approach does not seem to have a predicting power. For example it is unclear how to generalize the square lattice results to a different lattice. On the other hand the slave-rotor theory (see Sec.V) can reproduce all those results in a systematical way, and it is obviously can be applied to other lattices. In this section we will apply the slave-rotor theory on honeycomb lattice, following exactly the same route as in Sec.V, and discuss its XY $\leftrightarrow$ SC direct transition.

We again firstly present the minimal requirement of symmetries for microscopic models containing the XY $\leftrightarrow$ SC direct transition. In summary the symmetries are: charge- $U(1)$ ,  $S_z - U(1)$ ,  $PH$  (particle-hole),  $\mathcal{P}$  (reflection of the mirror along the diagonal direction of the hexagonal plaquette) and  $\mathcal{TR}$  ( $\mathcal{TR}$  is time-reversal). These transformations affect the electron operators as follows:

$$\begin{aligned} \text{charge-}U(1): c_{i\uparrow} &\rightarrow e^{i\theta} c_{i\uparrow} & c_{i\downarrow} &\rightarrow e^{i\theta} c_{i\downarrow} \\ S_z - U(1): c_{i\uparrow} &\rightarrow e^{i\theta/2} c_{i\uparrow} & c_{i\downarrow} &\rightarrow e^{-i\theta/2} c_{i\downarrow} \\ PH: c_{i\uparrow} &\rightarrow \eta_i c_{i\downarrow}^\dagger & c_{i\downarrow} &\rightarrow -\eta_i c_{i\uparrow}^\dagger \\ \mathcal{TR}: c_{i\uparrow} &\rightarrow c_{i\downarrow} & c_{i\downarrow} &\rightarrow -c_{i\uparrow} \\ \mathcal{P}: c_{i\uparrow} &\rightarrow c_{\mathcal{P}(i)\uparrow} & c_{i\downarrow} &\rightarrow c_{\mathcal{P}(i)\downarrow} \end{aligned} \quad (H1)$$

To describe the XY magnetic ordered phase on the honeycomb lattice by slave-rotor theory, we again assume that the bosonic chargon  $z$  are fully gapped, and the fermionic spinon  $f$  band structure to be TBI<sup>22</sup>:

$$\begin{aligned} H_f^{TBI} &= -t \sum_{\langle i,j \rangle} f_{i\sigma}^\dagger f_{j\sigma} + i \sum_{\langle\langle i,j \rangle\rangle} \lambda_{i,j} \left( f_{i\uparrow}^\dagger f_{j\uparrow} - f_{i\downarrow}^\dagger f_{j\downarrow} \right) \\ &+ h.c., \end{aligned} \quad (H2)$$

where  $\lambda_{ij} = \lambda \frac{\hat{d}_{jl} \times \hat{d}_{li} \cdot \hat{z}}{|\hat{d}_{jl} \times \hat{d}_{li}|} \equiv \nu_{ij} \lambda$ , and  $\hat{d}_{jl}, \hat{d}_{li}$  are the two bonds connecting site  $j$  and  $i$ ,  $\nu_{ij} = \pm 1$ . This band structure is the same as the Kane-Mele spin-hall insulator<sup>22</sup> if one replaces the spinon operator  $f$  by electron operator  $c$ . But the difference is that here the spinon  $f$  automatically couples with a dynamical 2+1D  $U(1)$  gauge field. Due to the "spin-hall" effect of the TBI band structure, we learn that the photon mode of the  $U(1)$  gauge field is actually the Goldstone mode of the XY magnet. Similar to the square lattice case, the low energy effective theory of the XY magnet has the form of Eq.(13). One can show that the microscopic symmetries Eq.(H1) ensure the correctness of this low energy effective theory.

The issue is to determine the XY and SC order patterns. We first study the XY order pattern. Is it ferromagnetic or anti-ferromagnetic? To answer this question we again perform two calculations both showing the order is AF. First we computed the matrix element ratio

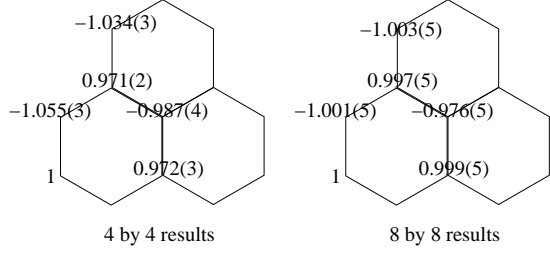


FIG. 15: We present the numerical result of the ratio of matrix elements  $\frac{\langle GS, 1\text{-flux} | P S_j^+ P | GS, 0\text{-flux} \rangle}{\langle GS, 1\text{-flux} | P S_j^+ P | GS, 0\text{-flux} \rangle}$  for the projected TBI wavefunction on 4 by 4 and 8 by 8 unit cell lattices on torus. We always fix site  $i$  to be the left-bottom one and show the result of site  $j$  on figure. The  $P|GS, 1\text{-flux}\rangle$  breaks physical translations and rotations since there are fluxes in the torus holes, and thus the magnitude of this ratio is not exactly one. But in the thermodynamic limit where the boundary condition is irrelevant, the magnitude of the ratio should approaches one, which seems to happen if one compares the 4 by 4 result and 8 by 8 result. The relative phases of the matrix element is exactly 0 for same sublattice and  $\pi$  for opposite sublattices. We choose hopping parameters  $\lambda/t = 0.1$  in these calculations, but the relative phases are found to be independent of choice of the parameters's value.

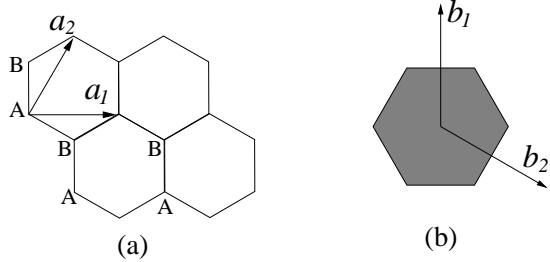


FIG. 16: (a) The honeycomb lattice in real space. The two sublattices are labeled by  $A$  and  $B$ .  $\mathbf{a}_1$  and  $\mathbf{a}_2$  are the two unit cell basis vectors. (b) The Brillouin zone of the honeycomb lattice. The vectors  $\mathbf{b}_1$  and  $\mathbf{b}_2$  are the two basis of the reciprocal lattice satisfying  $\mathbf{a}_i \cdot \mathbf{b}_j = \delta_{ij}$ .

to study the quantum number of monopoles of the  $U(1)$  gauge field (see Sec.F). We find the magnetic order is anti-ferromagnetic and in Fig. 15 we presented the matrix element ratio results.

Secondly we directly measure the spin-spin correlation function of the projected TBI wavefunction. We label the two sites in one honeycomb unit cell by  $A$  and  $B$  as shown in Fig.16, and define  $|\Psi_0\rangle = P|GS, 0\text{-flux}\rangle$ . The correlation functions that we measure are:

$$\begin{aligned} C^{AA}(\vec{r}) &= \langle S_A^x(\vec{r}) S_A^x(0) + S_A^y(\vec{r}) S_A^y(0) \rangle_{\Psi_0}, \\ C^{AB}(\vec{r}) &= \langle S_B^x(\vec{r}) S_A^x(0) + S_B^y(\vec{r}) S_A^y(0) \rangle_{\Psi_0}. \end{aligned} \quad (\text{H3})$$

Because the projected wavefunction is the simplest way to mimic the effect of the gauge fluctuations (i.e., the one-fermion-per-site constraint), we expect that this correlation function to show AF order.

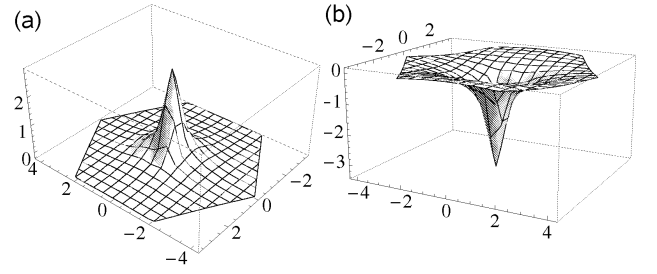


FIG. 17: For 8 by 8 unit cells, we fix hopping parameters  $t = 1$ ,  $\lambda = 0.1$  and plot Fourier transform of the real space spin spin correlation function  $\langle S^x(r) S^x(0) + S^y(r) S^y(0) \rangle$  of the projected wavefunction in the hexagonal Brillouin zone of the honeycomb lattice. (a) is the correlation function of the same sublattice  $C^{AA}$ . (b) is the correlation function of different sublattices  $C^{AB}$ . The large  $q = 0$  positive peak for  $C^{AA}$  and negative peak for  $C^{AB}$  is a strong evidence that this projected wavefunction is AF ordered.

We firstly present the projected wavefunction result for a fixed lattice size, namely 8 by 8 unit cells (see Fig.17). The momentum space peak at  $q = 0$  for Fourier transform of the XY spin correlation (positive for  $C^{AA}$  and negative for  $C^{AB}$ ) is a strong indication that the magnetic order is AF.

Next we present the finite size scaling study. When  $\lambda/t = 0$ , the projected wavefunction has two Dirac nodes and is expected to show power law scalings of the spin correlation function. We choose periodic boundary condition for difference system sizes  $L = 8, 10, 14, 16, 20, 22$  (Note that  $6N \times 6N$  lattice has nodal fermions, namely fermion modes right at the nodes. Thus we avoid those lattice sizes.), and compute the spin correlation functions  $C^{AA}$  and  $C^{AB}$  at the half way of the system sizes.

We checked that the projected wavefunctions that we used respect the full lattice space group symmetry. By the lattice space group symmetry, we find the three spin correlations at half system sizes for  $C^{AA}$ , namely  $C^{AA}(\frac{L\mathbf{a}_1}{2})$ ,  $C^{AA}(\frac{L\mathbf{a}_2}{2})$  and  $C^{AA}(\frac{L(\mathbf{a}_1+\mathbf{a}_2)}{2})$ , are related by symmetry transformation and thus identical. Here  $\mathbf{a}_1$  and  $\mathbf{a}_2$  are the real space unit cell basis of the honeycomb lattice as shown in Fig.16. On the other hand for  $C^{AB}$  we find  $C^{AB}(\frac{L\mathbf{a}_2}{2})$  and  $C^{AB}(\frac{L(\mathbf{a}_1+\mathbf{a}_2)}{2})$  are identical, but  $C^{AB}(\frac{L\mathbf{a}_1}{2})$  are different from them. Therefore we present the results of  $C^{AA}(\frac{L\mathbf{a}_1}{2})$ ,  $C^{AB}(\frac{L\mathbf{a}_2}{2})$  and  $C^{AB}(\frac{L\mathbf{a}_1}{2})$  in Fig.18(a). (Note that  $C^{AA}$  data are positive and  $C^{AB}$  data are negative, and we present the absolute values only.) We find

$$\lambda/t = 0: C(\vec{r}) \propto \frac{1}{|\vec{r}|^{1.89(2)}}. \quad (\text{H4})$$

Now we turn on  $\lambda$ . Based on the low energy effective theory (see text) we know the ground state should be long-range XY spin ordered. But by studying the projected wavefunction, we find the spin correlation function still have power law scaling. The scaling exponent,



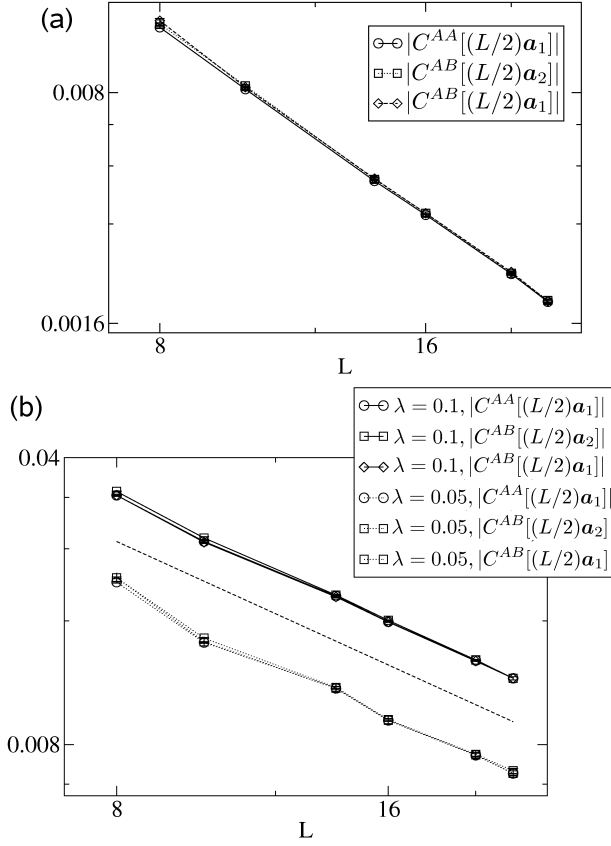


FIG. 18: We present the log-log plot of the finite size scaling of the spin-spin correlation functions for parameters  $t = 1$  and (a)  $\lambda = 0$  and (b)  $\lambda = 0.05$  and  $0.1$ . From (a), we find when  $\lambda/t = 0$  the scaling power law is  $|C| \propto \frac{1}{L^{1.89(2)}}$ . From (b) we also find power-law scalings for  $\lambda/t = 0.05$  and  $\lambda/t = 0.1$ , and the exponents for these two cases are the same up to statistical error, which is  $C \propto \frac{1}{L^{1.00(2)}}$ . The dashed line in (b) is the plot of  $C = \frac{0.2}{L}$ .

however, is strongly modified from the  $\lambda = 0$  value (see Fig.18(b)). We find

$$\lambda/t = 0.05, 0.1: C(\vec{r}) \propto \frac{1}{|\vec{r}|^{1.00(2)}}. \quad (\text{H5})$$

This means first the projected wavefunction fails to produce the true long-range correlation, and second the AF correlation is strongly enhanced with  $\lambda \neq 0$  projected wavefunction compared with the  $\lambda = 0$  one.

Now we study the SC order pattern. This is straightforward because we should simply condense  $z_1$  and  $z_2$  together. Deep in the SC phase the easy-plane condensation of  $z$ -boson can be achieved by doing replacement  $z_1 = \frac{1}{\sqrt{2}}e^{i\theta_1}$  and  $z_2 = \frac{1}{\sqrt{2}}e^{i\theta_2}$  in Eq. (28):

$$c_{i\uparrow} = \frac{1}{\sqrt{2}}(f_{i\uparrow}e^{i\theta_1} - \eta_i f_{i\downarrow}^\dagger e^{-i\theta_2}) \quad (\text{H6})$$

$$c_{i\downarrow} = \frac{1}{\sqrt{2}}(f_{i\downarrow}e^{i\theta_1} + \eta_i f_{i\uparrow}^\dagger e^{-i\theta_2}). \quad (\text{H7})$$

We can express  $f$  fermions in terms of the electron operator  $c$ :

$$f_{i\uparrow} = \frac{1}{\sqrt{2}}(c_{i\uparrow}e^{-i\theta_1} + \eta_i c_{i\downarrow}^\dagger e^{-i\theta_2}) \quad (\text{H8})$$

$$f_{i\downarrow} = \frac{1}{\sqrt{2}}(c_{i\downarrow}e^{-i\theta_1} - \eta_i c_{i\uparrow}^\dagger e^{-i\theta_2}) \quad (\text{H9})$$

Plugging these into Eq.(H2), the superconductor Hamiltonian is:

$$H^{SC} = t \sum_{\langle i,j \rangle} c_{i\alpha}^\dagger c_{j\alpha} + i\lambda \sum_{\langle\langle i,j \rangle\rangle} \nu_{ij} \eta_i e^{i(\theta_2 - \theta_1)} (c_{i\uparrow} c_{j\downarrow} + c_{i\downarrow} c_{j\uparrow}) + h.c. \quad (\text{H10})$$

If we absorb  $e^{i(\theta_2 - \theta_1)}$  into  $\lambda$  so that  $\lambda$  is complex, the full n.n.n. pairings are

$$(-)^i \nu_{ij} [i\lambda (c_{i\uparrow} c_{j\downarrow} + c_{i\downarrow} c_{j\uparrow}) + i\lambda^* (c_{i\uparrow}^\dagger c_{j\downarrow}^\dagger + c_{i\downarrow}^\dagger c_{j\uparrow}^\dagger),] \quad (\text{H11})$$

these are  $f$ -wave triplet pairings with  $S_z = 0$ . Note that this  $f$ -wave SC is fully gapped (its spectrum is the same as TBI). Therefore we show that there is a direct AF  $\leftrightarrow$   $f$ -wave SC transition on honeycomb lattice, whose low energy effective theory is again the easy-plane limit of NCCP<sup>1</sup>.

Finally we remark that there are zero modes in the vortex cores of the AF and  $f$ -wave SC phases by solving the BdG equations. We already presented the mean-field Hamiltonian of the SC phase in Eq.(H10). To write down the AF mean-field Hamiltonian one should study which terms are allowed by symmetry (in AF phase, the good symmetries are charge- $U(1)$ ,  $PH$ ,  $\mathcal{P}$  and  $e^{i\pi S_z} \circ \mathcal{TR}$ ). The simplest AF mean-field Hamiltonian consistent with symmetries is:

$$H^{XY} = t \sum_{\langle ij \rangle} c_{i\alpha}^\dagger c_{j\alpha} + \eta_i \sum_i (M^* c_{i\uparrow}^\dagger c_{i\downarrow} + M c_{i\downarrow}^\dagger c_{i\uparrow}). \quad (\text{H12})$$

where  $M$  is the on-site magnetization.

When the order parameters are small both Eq.(H10) and Eq.(H12) are in the Dirac limit. The AF side BdG equation has already been solved by Herbut<sup>40</sup>. And one can show that the SC side BdG equation turns out to be the same as the AF side BdG equation after appropriate rotations. One can show that the whole analysis on the square lattice, namely zero modes  $\rightarrow$  vortex carry quantum number  $\rightarrow$  direct transition, also carries through on the honeycomb lattice and reproduce the same low energy effective theory as the one given by slave-rotor theory.

- 
- <sup>1</sup> T. Senthil and P. A. Lee, Phys. Rev. B **71**, 174515 (2005).
  - <sup>2</sup> T. Senthil, A. Vishwanath, L. Balents, S. Sachdev, and M. P. A. Fisher, Science **303**, 1490 (2004).
  - <sup>3</sup> N. Read and S. Sachdev, Phys. Rev. B **42**, 4568 (1990).
  - <sup>4</sup> L. Balents, L. Bartosch, A. Burkov, S. Sachdev, and K. Sengupta, Phys. Rev. B **71**, 144508 (2005).
  - <sup>5</sup> T. Grover and T. Senthil, Phys. Rev. Lett. **98**, 247202 (2007).
  - <sup>6</sup> A. A. Burkov and L. Balents, Phys. Rev. B **72**, 134502 (2005).
  - <sup>7</sup> T. Grover and T. Senthil, Phys. Rev. Lett. **100**, 156804 (2008).
  - <sup>8</sup> F. F. Assaad, M. Imada, and D. J. Scalapino, Phys. Rev. Lett. **77**, 4592 (1996).
  - <sup>9</sup> O. I. Motrunich and A. Vishwanath, Phys. Rev. B **70**, 075104 (2004).
  - <sup>10</sup> Z. Y. Weng, D. N. Sheng, and C. S. Ting, Phys. Rev. Lett. **80**, 5401 (1998).
  - <sup>11</sup> S.-P. Kou, X.-L. Qi, and Z.-Y. Weng, Phys. Rev. B **71**, 235102 (2005).
  - <sup>12</sup> Z.-Y. Weng, International Journal of Modern Physics B **21**, 773 (2007).
  - <sup>13</sup> B. S. A.B. Kuklov, N.V. Prokofev and M. Troyer, Annals of Physics **321**, 1602 (2006).
  - <sup>14</sup> A. W. Sandvik, Phys. Rev. Lett. **98**, 227202 (2007).
  - <sup>15</sup> R. G. Melko and R. K. Kaul, Phys. Rev. Lett. **100**, 017203 (2008).
  - <sup>16</sup> O. I. Motrunich and A. Vishwanath (2008), URL [arXiv.org:0805.1494](https://arxiv.org/abs/0805.1494).
  - <sup>17</sup> A. B. Kuklov, M. Matsumoto, N. V. Prokof'ev, B. V. Svistunov, and M. Troyer (2008), URL [arXiv.org:0805.4334](https://arxiv.org/abs/0805.4334).
  - <sup>18</sup> I. Affleck and J. B. Marston, Phys. Rev. B **37**, 3774 (1988).
  - <sup>19</sup> P. Lee, N. Nagaosa, and X.-G. Wen, Rev. Mod. Phys. **78**, 17 (2006).
  - <sup>20</sup> X. G. Wen, F. Wilczek, and A. Zee, Phys. Rev. B **39**, 11413 (1989).
  - <sup>21</sup> D. J. Thouless, M. Kohmoto, M. P. Nightingale, and M. den Nijs, Phys. Rev. Lett. **49**, 405 (1982).
  - <sup>22</sup> C. L. Kane and E. J. Mele, Phys. Rev. Lett. **95**, 226801 (2005).
  - <sup>23</sup> Y. Ran, A. Vishwanath, and D.-H. Lee (2008), URL [arXiv.org:0801.0627](https://arxiv.org/abs/0801.0627).
  - <sup>24</sup> C. Dasgupta and B. I. Halperin, Phys. Rev. Lett. **47**, 1556 (1981).
  - <sup>25</sup> M. P. A. Fisher and D. H. Lee, Phys. Rev. B **39**, 2756 (1989).
  - <sup>26</sup> G. Baskaran, Z. Zou, and P. Anderson, Solid State Commun. **63**, 973 (1987).
  - <sup>27</sup> L. B. Ioffe and A. I. Larkin, Phys. Rev. B **39**, 8988 (1989).
  - <sup>28</sup> D. A. Ivanov and P. A. Lee, Phys. Rev. B **68**, 132501 (2003).
  - <sup>29</sup> A. M. Polyakov, Nuclear Physics B **120**, 429 (1977).
  - <sup>30</sup> S.-S. Lee and P. A. Lee, Phys. Rev. Lett. **95**, 036403 (2005).
  - <sup>31</sup> S. Florens and A. Georges, Phys. Rev. B **70**, 035114 (2004).
  - <sup>32</sup> M. Hermele, T. Senthil, and M. P. A. Fisher, Phys. Rev. B **72**, 104404 (2005).
  - <sup>33</sup> X.-G. Wen and P. A. Lee, Phys. Rev. Lett. **76**, 503 (1996).
  - <sup>34</sup> B. I. Halperin, T. C. Lubensky, and S.-k. Ma, Phys. Rev. Lett. **32**, 292 (1974).
  - <sup>35</sup> S. Sachdev, *Quantum Phase Transitions* (Cambridge University Press, Cambridge U.K., 1999).
  - <sup>36</sup> C.-Y. Hou, C. Chamon, and C. Mudry, Phys. Rev. Lett. **98**, 186809 (2007).
  - <sup>37</sup> M. Hermele, Phys. Rev. B **76**, 035125 (2007).
  - <sup>38</sup> Y. Ran, W.-H. Ko, P. A. Lee, and X.-G. Wen (2007), URL [arXiv.org:0710.4574](https://arxiv.org/abs/0710.4574).
  - <sup>39</sup> X.-G. Wen, Phys. Rev. B **65**, 165113 (2002).
  - <sup>40</sup> I. F. Herbut, Phys. Rev. Lett. **99**, 206404 (2007).